Instabilities and transition in the GeoFlow experiment on ISS: Quasi-stationary and chaotic convection in low rotating spherical shells

B. Futterer and C. Egbers

Brandenburg University of Technology Cottbus, Germany

12th EUROMECH European Turbulence Conference
Marburg, Sept. 7–10 2009

funded by: German Aerospace Center e.V. (DLR), Grant number 50 WM 0122, 50 WM 0822, European Space Agency (ESA), Grant number AO99-049, 18950/05/NL/VJ

Outline

Spherical Rayleigh-Bénard convection in self-gravitating force field, superposition of rotation

- radial gravity force (dielectrophoretic)
  - I. Yavorskaya, N. Fomina, Y. Belyaev, *A simulation of central-symmetry convection in microgravity conditions,* Acta Astronaut. 11 (1984), 179–183
  - J. Hart, G. Glatzmaier, J. Toomre *Space-laboratory experiments and numerical simulations of thermal convection in a rotating hemispherical shell with radial gravity,* J. Fluid Mech. 173 (1986), 512–544
- spherical shell convection
  - H.F. Busse, *Patterns of convection in spherical shells,* J. Fluid Mech. 72 (1975), 67–85
- convection in rotating shells (recent)
  - F.H. Busse, *Convective flows in rapidly rotating spheres and their dynamo action,* Phys. Fluids 14 (2002), 1301–1313
  - R. Simitev & F.H. Busse, *Patterns of convection in rotating spherical shells,* New J. of Physics 5 (2003), 97.1–97.20
  - R. Simitev & F.H. Busse, *Prandtl-number dependence of convection-driven dynamos in rotating spherical shells,* J. Fluid Mech. 532 (2005), 365–388
  - N. Gillet, D. Brito, D. Jault, H.-C. Nataf, *Experimental and numerical studies of convection in a rapidly rotating spherical shell,* J. Fluid Mech. 580 (2007), 83–121
  - F. Garcia, J. Sanchez, M. Net, *Antisymmetric polar modes of thermal convection in rotating spherical fluid shells at high Taylor numbers,* Phys. Rev Lett. 101 (2008), 365–388

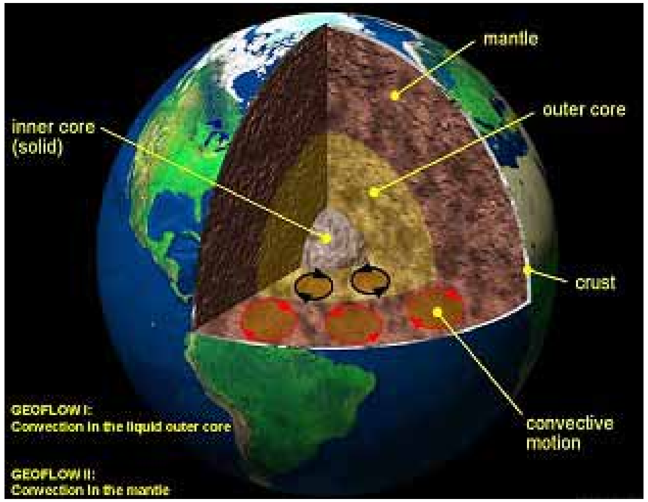

Earth's interior's scaled to spherical shells

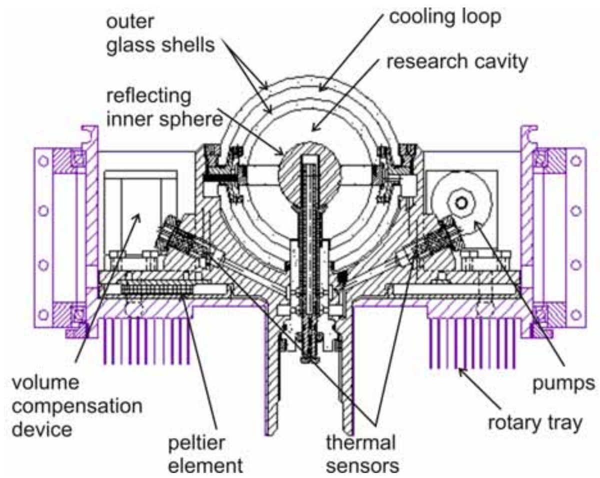

Sketch of experimental shell system

Objectives of GeoFlow **experiment**: spherical Rayleigh-Bénard convection in self-gravitating force field, superposition of rotation

- radial gravity force by high voltage potential between inner and outer spherical shells
  (dielectrophoretic effect in microgravity environment on ISS)
- fully spherical shell with radius ratio of $\eta = 0.5$,
  filled with dielectric fluid of $Pr \approx 65$
- spherical shell convection for non-rotating case
- convection in rotating spherical shells
- Rayleigh number $Ra_{centr} \approx 2 \cdot 10^5$ ($Ra \sim \Delta T$),
  Taylor number $Ta \approx 10^7$ ($Ta \sim f$)
- non-magnetic experiment

characterization

- flow patterns of convection for non-rotating and rotating spherical shells
- identification of stability of co-existing modes ($Ta = 0$)
- identification of travelling waves (Ta low)
- change of sign for drift velocities (Ta intermediate)
- up to columnar cells at the tangent cylinder (Ta high)

Non-dimensional Boussinesq equations for dielectric convection in spherical shells

$$\nabla \cdot \mathbf{U} = 0$$

$$Pr^{-1}\left[\frac{\partial \mathbf{U}}{\partial t} + (\mathbf{U}\cdot\nabla)\mathbf{U}\right] = -Pr^{-1}\nabla p + \nabla^2\mathbf{U} + Ra_{centr}\cdot\frac{\eta^2}{(1-\eta)^2}\cdot\frac{1}{r^5}\,T\,\hat{\mathbf{e}}_r$$
$$-\sqrt{Ta}\,\hat{\mathbf{e}}_z \times \mathbf{U} + \widetilde{Ra}\,T\,r\sin\theta\,\hat{\mathbf{e}}_{eq}$$

$$\frac{\partial T}{\partial t} + \mathbf{U}\cdot\nabla T = \nabla^2 T$$

no-slip boundary conditions for velocity $\mathbf{U}$, temperature fixed $T(\eta) = 1$, $T(1) = 0$; rotating reference frame, scaled to outer spherical radius

Parameters

radius ratio	$\eta = \frac{r_i}{r_o}$
Prandtl number	$Pr = \frac{\nu}{\kappa}$
Rayleigh number	$Ra_{centr} = \frac{2\epsilon_0\epsilon_r\gamma}{\rho\nu\kappa}\,V^2_{\mathrm{rms}}\,\Delta T$
Taylor number	$Ta = \left(\frac{2\Omega r_o^2}{\nu}\right)^2$
additional factor	$\widetilde{Ra} = \frac{\alpha\Delta T}{4}\,Ta\,Pr$

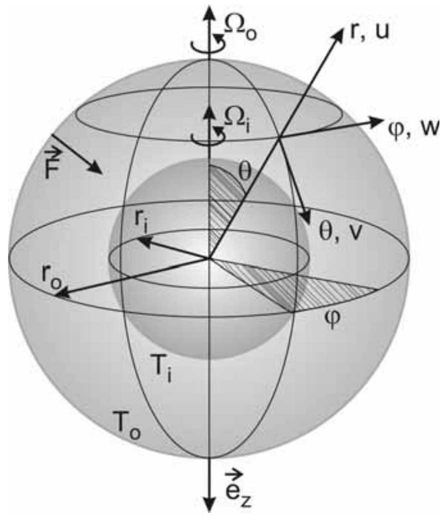

Experimental constraints

					GeoFlow	outer core	mantle
gap	$r_o - r_i [mm]$	13.5	$\rightarrow$	η	0.5	0.37	0.55
viscosity	$\nu [m/s^2]$	$5 \cdot 10^{-6}$	$\rightarrow$	Pr	64.64	0.1-1.0	∞, $F(T,z)$
voltage temperature	$V_{rms}[kV]$ $\Delta T [K]$	10 ≤ 10	$\}$	Ra_{centr}	$\leq 1.4 \cdot 10^5$	$>10^{29}$	$10^6 - 10^8$
rotation	$f[Hz]$	≤ 2	$\rightarrow$	Ta	$\leq 1.3 \cdot 10^7$	10^{30}	$<< 1$

Spectral method for numerical simulation

- decomposition of primary variables into poloidal and toroidal parts
- decomposition of these into Chebyshev polynomials and spherical harmonics
- solving equations for spectral coefficients
  $e(r, \theta, \varphi, t) = \sum_{m=0}^{M} \sum_{\ell=m'}^{L} \sum_{k=1}^{K} e_{k\ell m} T_{k-1}(x) P_\ell^{|m|}(\cos\theta) e^{im\phi}$
- truncation with (K,L,M)=(30,60,20)
- R. Hollerbach, *A spectral solution of the magneto-convection equations in spherical geometry*, Int. J. Numer. Meth. Fluids 32 (2000), 773–797
- global variables
  $Nu = -r^2 \frac{r_o - r_i}{r_i r_o} \frac{\partial T}{\partial r} \rightarrow Nu_i = -\frac{r_i}{r_o}(r_o - r_i)\frac{\partial T}{\partial r}$
  $E_{kin} = 0.5 \cdot \int (u_r^2 + u_\theta^2 + u_\phi^2) \cdot r^2 \, sin(\theta) \, dr \, d\theta \, d\phi$

Flow modes of the lower limit: non-rotating case $Ta = 0$

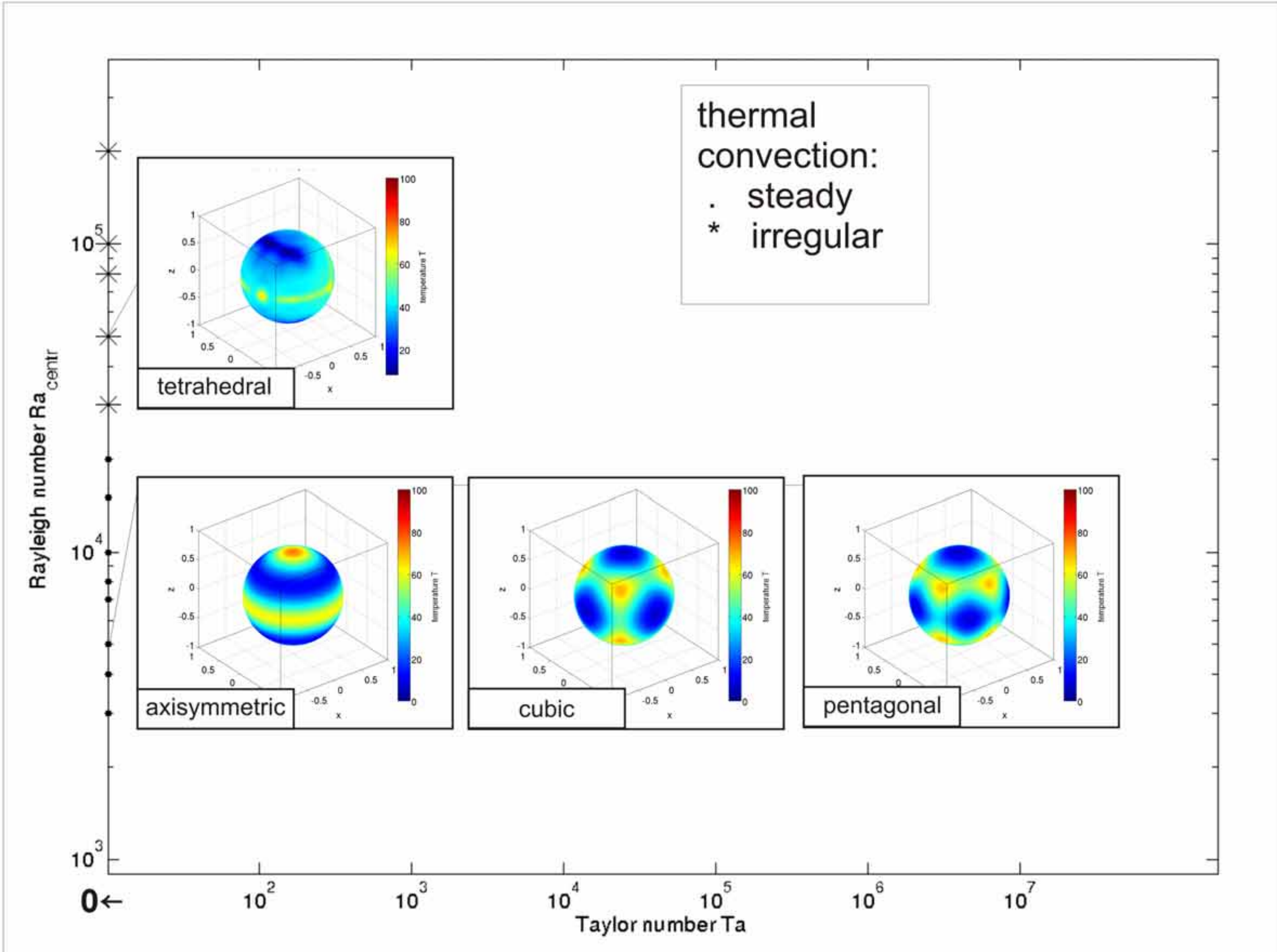

Patterns of convection:
Visualization of temperature field in radial direction, red color corresponds to hot up-flow and blue color to cold discharge.
Co-existing modes (K. Bergemann, L. Tuckerman, F. Feudel, *GeoFlow: On symmetry-breaking bifurcations of heated spherical shell convection,* J. Phys.: Conf. Ser. **137** (2008), 012027 (4pp)).

Flow modes of the higher limit: rotating case $Ta \neq 0$

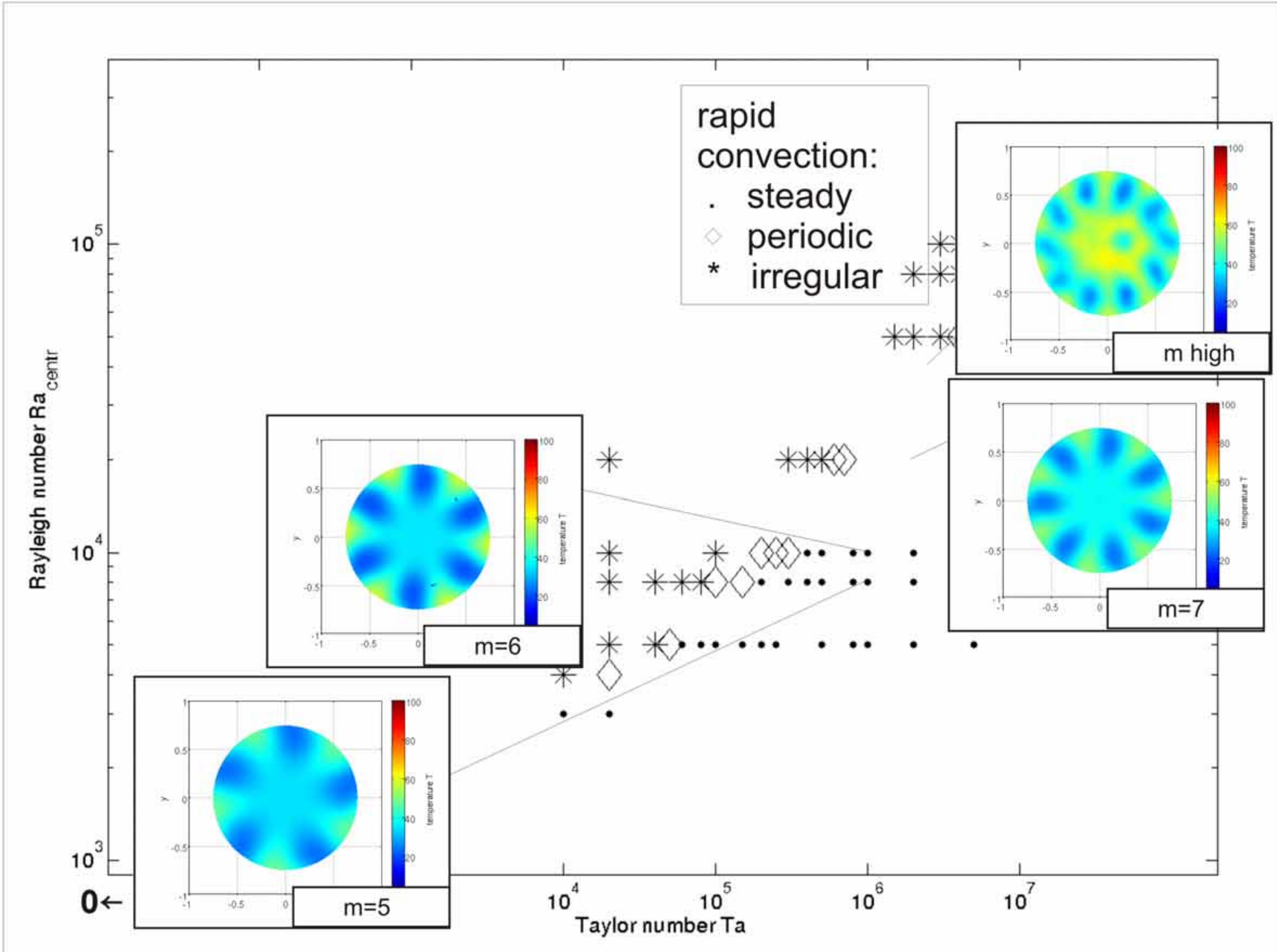

Patterns of convection:
Visualization of temperature field, view at the top of the sphere, i.e. the middle of the image is the ‘polar’ region.
Increase of mode number (V. Travnikov, R. Hollerbach, C. Egbers, *The GEOFLOW experiment on ISS. Part II: Numerical simulation*, Adv. Space Res. 32 (2003), 181–189).

Dynamics of low rotating spherical shell convection I

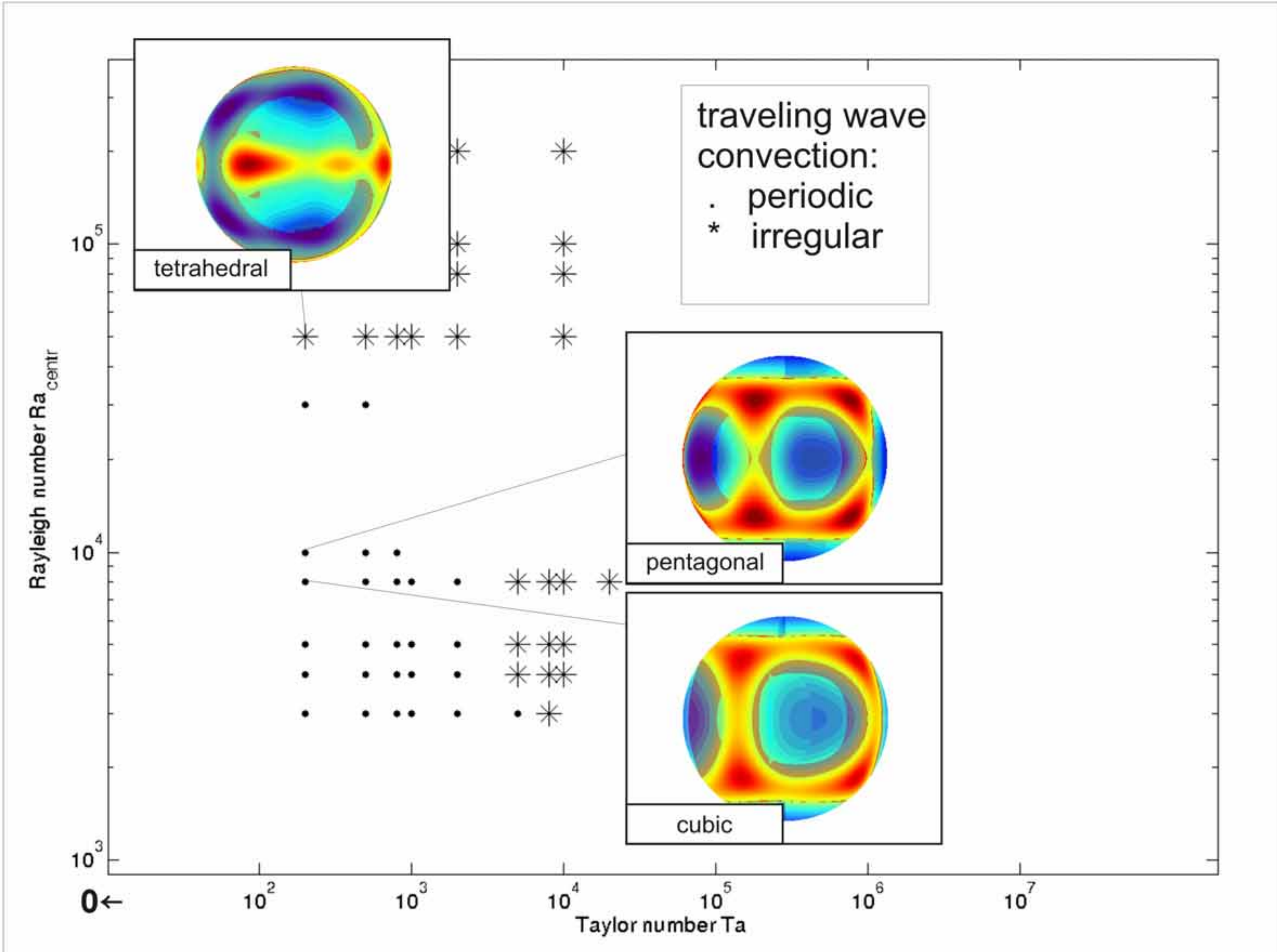

Patterns of convection:
Visualization of radial velocity field, red color corresponds to positive and blue color to negative direction of flow.
Modes as in the non-rotating regime.

Example: $Ta = 2 \cdot 10^2$

parameter Ra_{centr}	$v_r(r)$	$v_p(t)$	variables Nu, E_{kin}	coeff.
$3 \cdot 10^4$	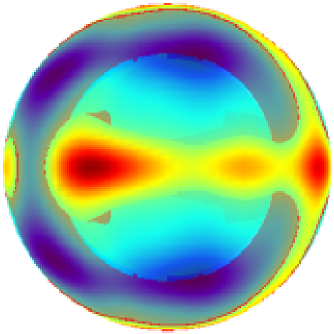	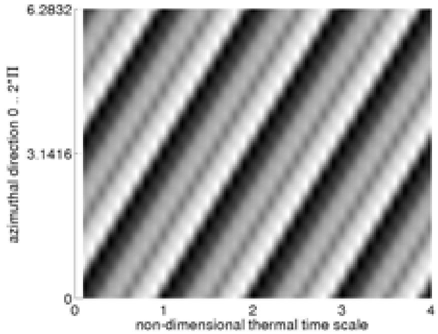	const.	periodic
$1 \cdot 10^4$	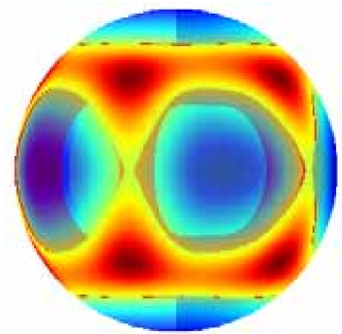	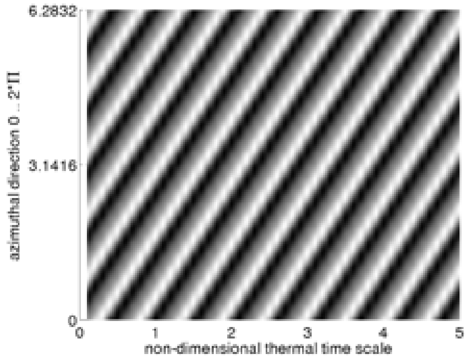	const.	periodic
$5 \cdot 10^3$	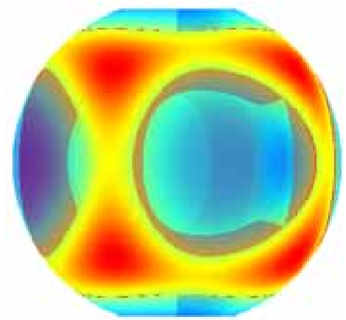	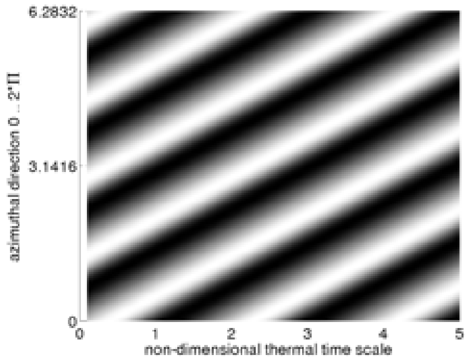	const.	periodic

Dynamics of low rotating spherical shell convection II

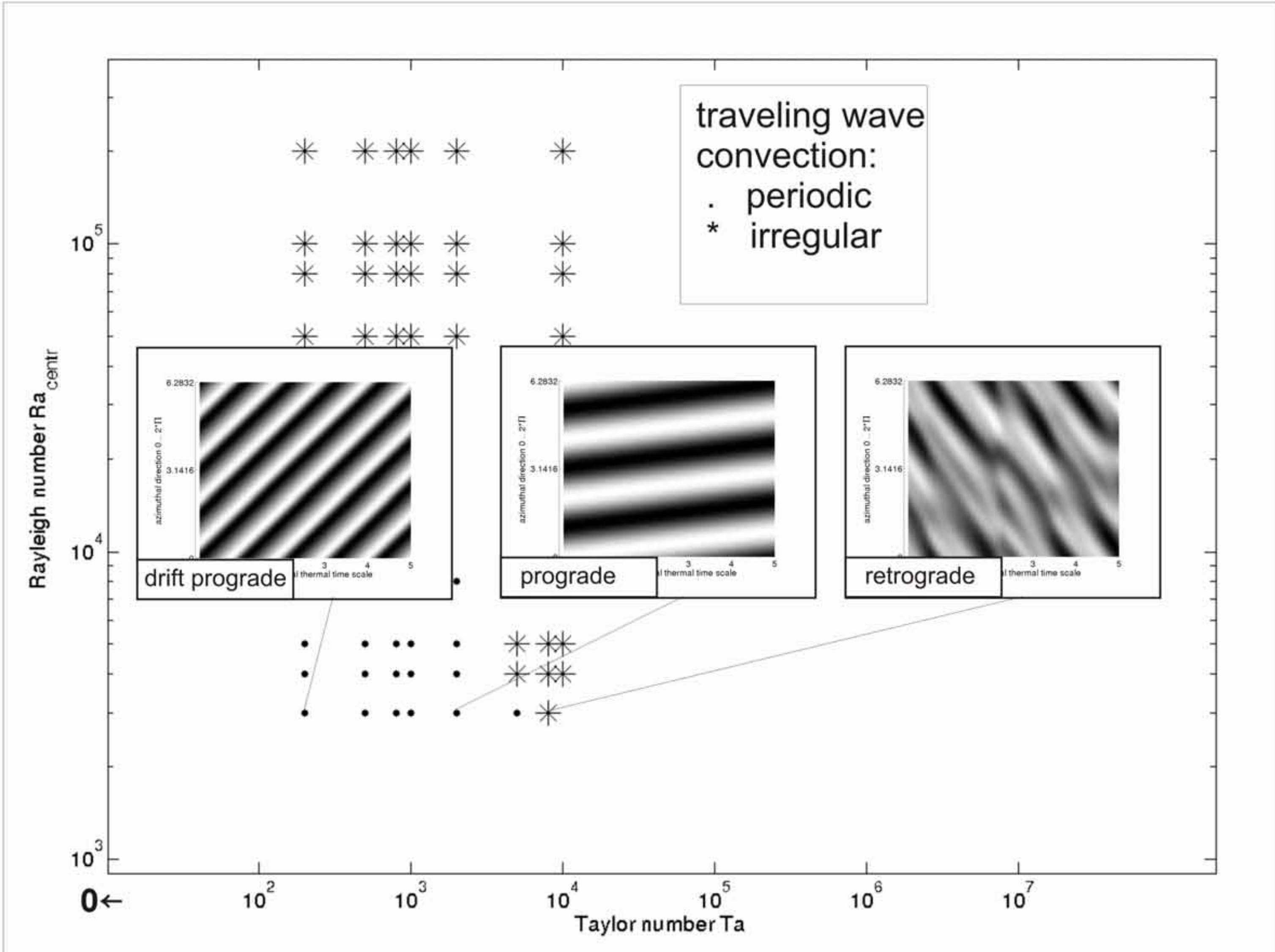

Space time plots of azimuthal velocity component: change of sign for drift velocity, also predicted by means of stability analysis (Travnikov et. al, 2003).

Example: $Ra = 3 \cdot 10^3$

param.			
Ta	$2 \cdot 10^2$	$2 \cdot 10^3$	$8 \cdot 10^3$
	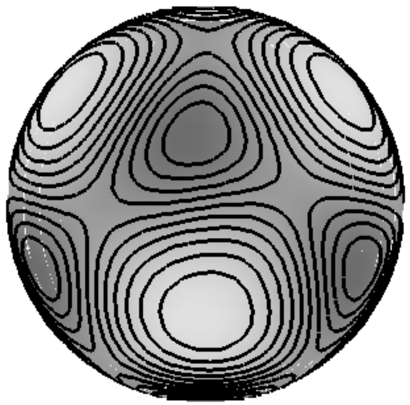	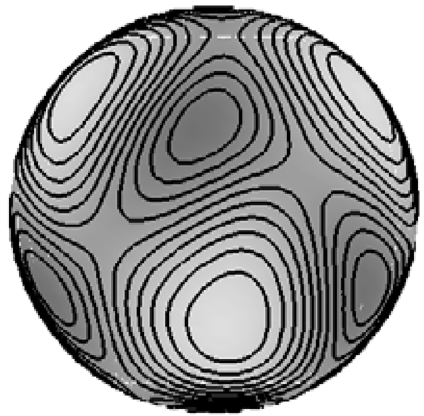	
Nu, E_{kin}	const.	const.	irregular
coeff.	periodic	quasi-periodic	irregular

Pattern of convection by visualization of temperature field in radial direction with view from side. Isolines demonstrate character of the pattern. Dark shading shows hot up-flow.

Summary

- GeoFlow
  - spherical Rayleigh-Bénard convection experiment in self-gravitating force field
  - microgravity environment of COLUMBUS on ISS
  - superposition of rotation
  - rotating regimes from $Ta = 0$ via low, intermediate up to rapid
- dynamics for low rotating regime
  - comparable to $Ta = 0$:
    - coexisting of several modes (axisymmetric, cubic, pentagonal)
    - transition from quasi-stationary to irregular flow with remnant tetrahedral symmetry
  - intermediate regime
    - change of sign for drift
    - prograde $\rightarrow$ retrograde

Outlook

- comparison with experimental data

State of the art: spherical Rayleigh-Bénard convection in self-gravitating force field, superposition of rotation

- radial gravity force by dielectrophoretic effect in microgravity environment
  - Yavorskaya et al. *A simulation of central-symmetry convection in microgravity conditions.* Acta Astronautica 11 (1984), 179–183
  - Hart et al. *Space-laboratory experiments and numerical simulations of thermal convection in a rotating hemispherical shell with radial gravity.* J. Fluid Mech. 173 (1986), 512–544
- spherical shell convection for non-rotating case
  - H.F. Busse. *Patterns of convection in spherical shells.* J. Fluid Mech. 72 (1975), 67–85
- convection in rotating spherical shells
  - A. Tilgner & F.H. Busse. *Finite-amplitude convection in rotating spherical shells.* J. Fluid Mech. 332 (1997), 359–376
  - F.H. Busse. *Convective flows in rapidly rotating spheres and their dynamo action.* Phys. Fluids 14 (2002), 1301–1313
  - R. Simitev & F.H. Busse. *Patterns of convection in rotating spherical shells.* New J. of Physics 5 (2003), 97.1–97.20
  - R. Simitev & F.H. Busse. *Prandtl-number dependence of convection-driven dynamos in rotating spherical shells.* J. Fluid Mech. 532 (2005), 365–388
  - N. Gillet, D. Brito, D. Jault, H.-C. Nataf. *Experimental and numerical studies of convection in a rapidly rotating spherical shell.* J. Fluid Mech. 580 (2007), 83–121
  - F. Garcia, J. Sanchez, M. Net. *Antisymmetric polar modes of thermal convection in rotating spherical fluid shells at high Taylor numbers.* Phys. Rev Lett. 101 (2008), 365–388

State of the art: spherical Rayleigh-Bénard convection in self-gravitating force field, superposition of rotation

- radial gravity force by dielectrophoretic effect in microgravity environment
  - theoretical discussion of central-symmetry convection in spherical layers under dielectrophoretic force in microgravity conditions
    $\mu = 0.5 \ldots 0.9$, $Pr = 15 \ldots 1020$, $Ra \approx 10^7$, $Ta = 0$
  - Spacelab 3 experiment for thermally driven circulations within rotating hemispherical shell
    $\mu = 0.73$, $Pr = 8.4$, $Ra \approx 10^6$, $Ta = 6 \cdot 10^5$

- spherical shell convection for non-rotating case
  - pattern of motion in convectively unstable system with spherical geometry
    $l = 4$ is responsible for the onset of convection

- convection in rotating spherical shells
  - drifting waves, time-dependent convection, heat transport
    $\mu = 0.4$, $Pr = 0.01 \ldots 10$, $Ra \approx 3 \cdot 10^5$, $Ta = 10^6$
  - Coriolis force, Rossby waves in centrifugally driven convection in rotating annulus, convection in rotating self-gravitating spherical shells
    $\mu = 0.4$, $Pr = 0.025 \ldots 1$, $Ra \approx 10^6$, $Ta \approx 10^4$
  - patterns of convection in internally heated convection, amplitude vascillations and spatial modulations of convective columns
    $\mu = 0.4$, $Pr = 0 \ldots 100$, $Ra \approx 10^6$, $Ta \approx 10^4$
  - low *Pr* promote dynamo action, high *Pr* number fluids influence on dynamo action
    $\mu = 0.4$, $Pr = 0.025 \ldots 20$, $Ra \approx 10^6$, $Ta \approx 10^5$
  - experiment with cylinder in the sphere
    $\mu = 0.36$, $Pr = 7$, $Ra \approx 10^6$, $Ta \approx 10^6$
  - onset of convection
    $\mu = 0.4$, $Pr = 0.01$, $Ra \approx 10^6$, $Ta \approx 10^{11}$

Coulomb force

- charged particle in electric field $\mathbf{E}$
- $\mathbf{F_C}(\mathbf{r}) = q\ \mathbf{E}$
- much stronger than dielectrophoretic force
- suppressed by using high-frequency AC voltage ($T_{el} \ll \tau$, τ – relaxation time of free particle)

Dielectrophoretic force

- due to polarisation of medium in electric fields (local dipoles)
- $\mathbf{F_D}(\mathbf{r}) = \frac{1}{2}\mathbf{E}^2(\mathbf{r})\nabla\epsilon$
- acting as a ponderomotive force only in geometrically inhomogeneous field
- resulting movement only for dieletric inhomogenous media
- depends on gradient of $\mathbf{E}$, not sign
- spherical geometry: $\mathbf{F_D}(\mathbf{r}) \sim \mathbf{1/r^5}$
- acts as central force field (comparable to gravity)

GeoFlow constraints ...

- spherical shell system is geometrically inhomogenous
- experimental fluid is dielectric homogenous

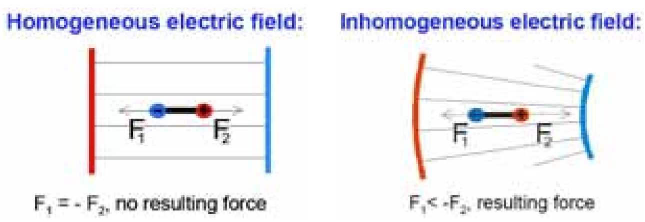

Setting up high voltage → acceleration due to dielectric force field

$$\mathbf{g_e} = \frac{1}{2\rho}\epsilon\epsilon_r \nabla |\mathbf{E}|^2 \quad \text{with} \quad \mathbf{E} = \frac{1}{r^2}\frac{r_i r_o}{r_o - r_i} V_0 \sin(\omega t)\hat{\mathbf{e}}_r$$

$$g_e = \frac{2\epsilon_0\epsilon_r}{\rho}\left(\frac{r_i r_o}{r_o - r_i}\right)^2 V_{rms}^2 \frac{1}{r^5}$$

ε_0 - dielectric constant, ε_r - relative permittivity, ρ - density, V_{rms} - voltage

GeoFlow specific values . . .

$$\epsilon_0 = 8.854 \cdot 10^{-12}\ {}^{As}/_{Vm}, \quad \epsilon_r = 2.7,$$

$$\rho = 920\ {}^{kg}/_{m^3},$$

$$d = r_o - r_i = 27\ mm - 13.5\ mm = \ 13.5\ mm,$$

$$V_{rms} = 10\ kV$$

$$\rightarrow g_e|_{r_o} \approx 10^{-1} m/s^2 \qquad \text{compared to} \quad g \approx 10^1 m/s^2$$

→ microgravity conditions required!

Timeseries for identification of time-dependencies in numerical solutions: global variable of kinetic energy

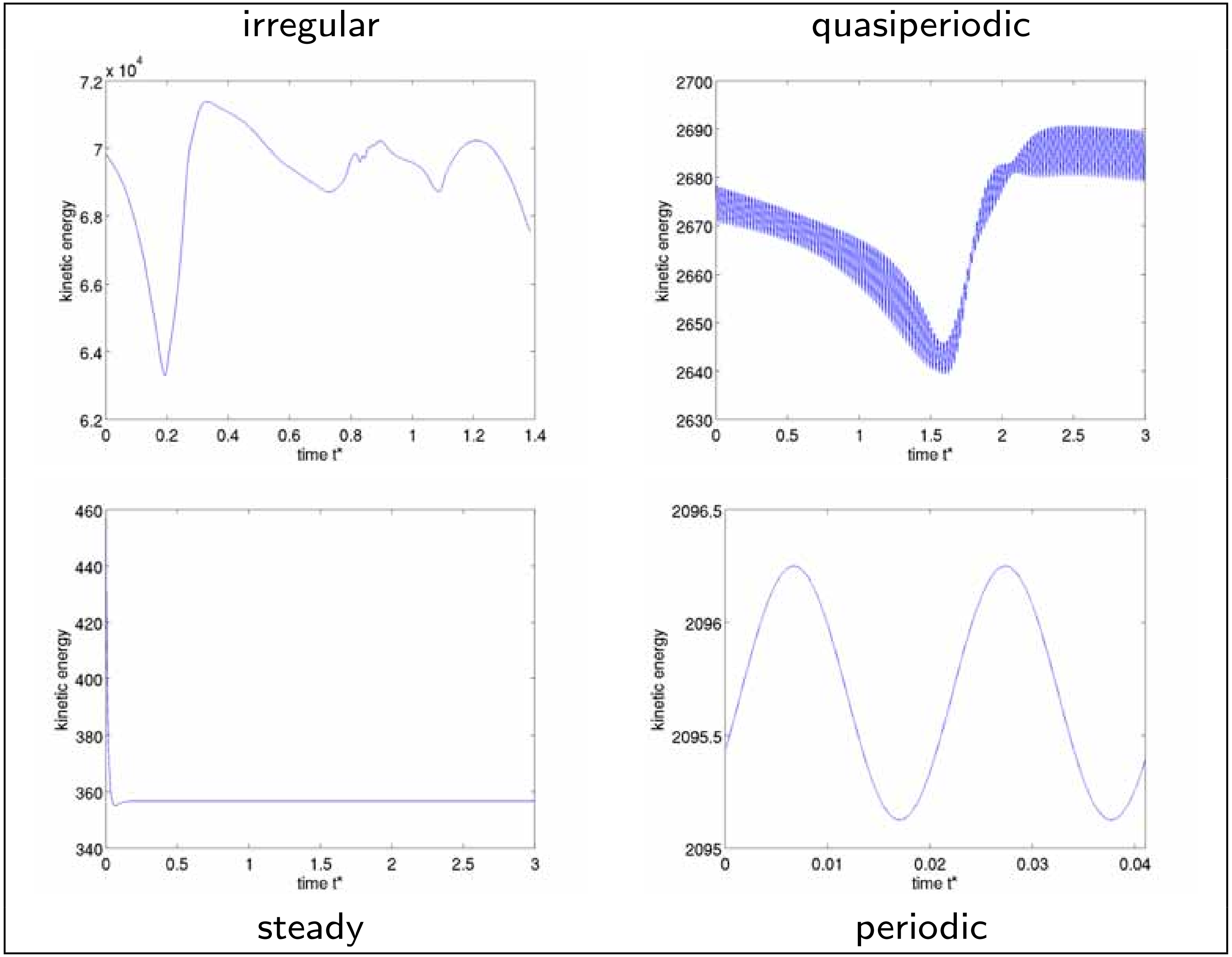

Timeseries for identification of time-dependencies in numerical solutions: global variables of kinetic energy and Nusselt number, local variables of spectral coefficient: $Ra_{centr} = 4 \cdot 10^3$, $Ta = 5 \cdot 10^2$

$E_{kin} = 230$	spect. coeff.
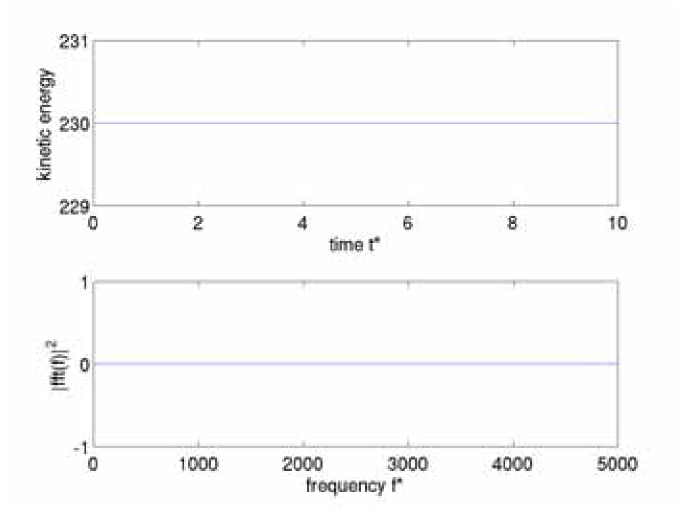	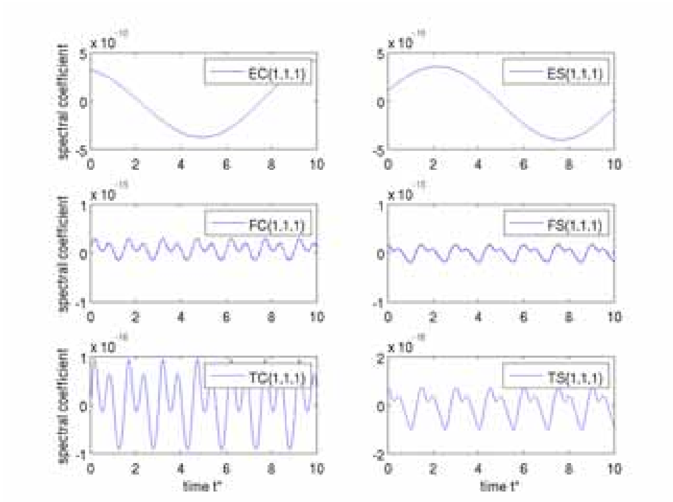
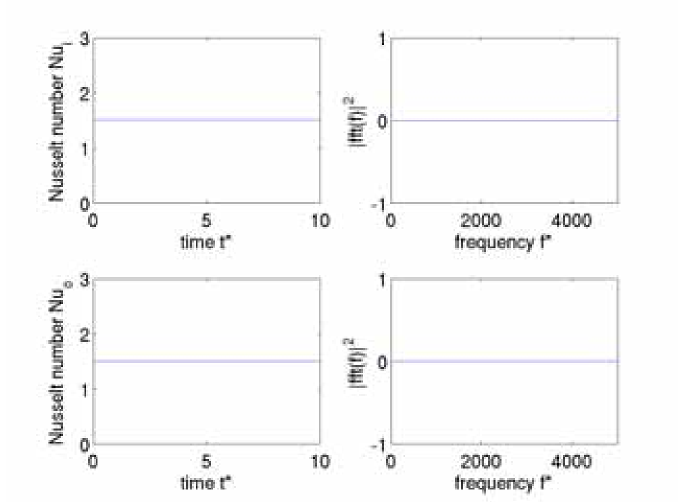	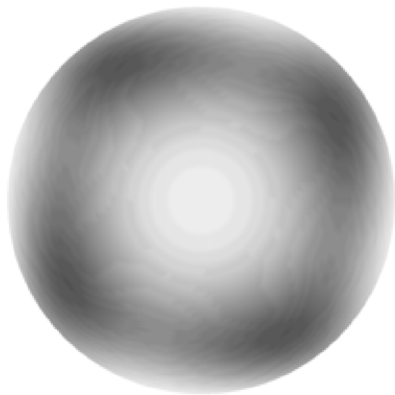
$Nu = 1.50369$	temp. pattern

History of simulation work for GeoFlow

- Stability analysis for both cases $Ta = 0$ (determination of onset of convection) and $Ta \neq 0$ (influence of centrifugal force, modes of instabilities)
  - V. Travnikov, R. Hollerbach, C. Egbers, *The GEOFLOW experiment on ISS. Part II: Numerical simulation*, Adv. Space Res. 32 (2003), 181–189
  - V. Travnikov, *Thermische Konvektion im Kugelspalt unter radialem Kraftfeld*, Dissertation, Cuvillier Verlag Göttingen, 2004
- Bifurcation analysis (influence of different force fields in geo-/astrophysical framework)
  - P. Beltrame, V. Travnikov, M. Gellert, C. Egbers, *GEOFLOW: Simulation of convection in a spherical gap under central force field*, Nonlinear Processes in Geophysics, 13, 1-11
- Path following analysis (determination of stable and unstable solutions for stationary states for case $Ta = 0$)
  - K. Bergemann, L. Tuckerman, F. Feudel, *GeoFlow: On symmetry-breaking bifurcations of heated spherical shell convection*, J. Phys.: Conf. Ser. **137** (2008), 012027 (4pp)
- Direct numerical simulations (fluid flow and temperature field, calculation of interferograms)
  - M. Gellert, P. Beltrame, C. Egbers, *The GeoFlow experiment - spherical Rayleigh-Bénard convection under the influence of an artificial central force field*, J. Phys.: Conf. Ser. 14 (2005), 157-161
  - B. Futterer, M. Gellert, Th. von Larcher, C. Egbers, *Thermal Convection in rotating spherical shells: An experimental and numerical approach within GeoFlow*, Acta Astronautica 62 (2008), 300–307
  - B. Futterer, R. Hollerbach, C. Egbers, *Geoflow: 3D numerical simulation of supercritical thermal convective states*, J. Phys.: Conf. Ser. **137** (2008), 012026 (5pp)

Linear analysis for $Ta = 0$

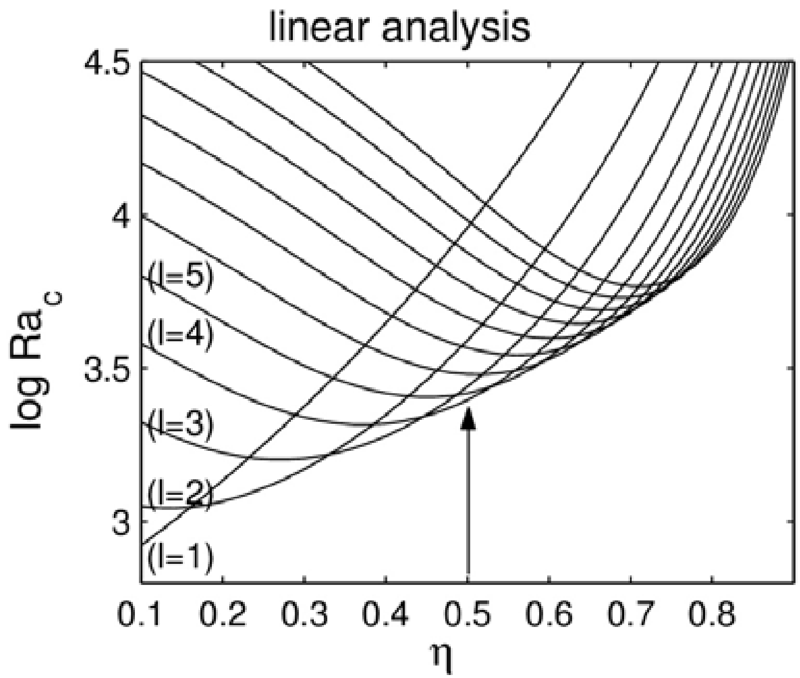

- critical Ra_{centr} for onset of convection independent on Pr
- larger $\eta \rightarrow$ larger critical mode l

Source: V. Travnikov, C. Egbers, R. Hollerbach, *The GEOFLOW experiment on ISS. Part II: Numerical simulation*, Adv. Space Res. 32 (2003), 181–189
V. Travnikov: *Thermische Konvektion im Kugelspalt unter radialem Kraftfeld*, Dissertation, Cuvillier Verlag Göttingen, 2004

Linear analysis for $Ta \neq 0$

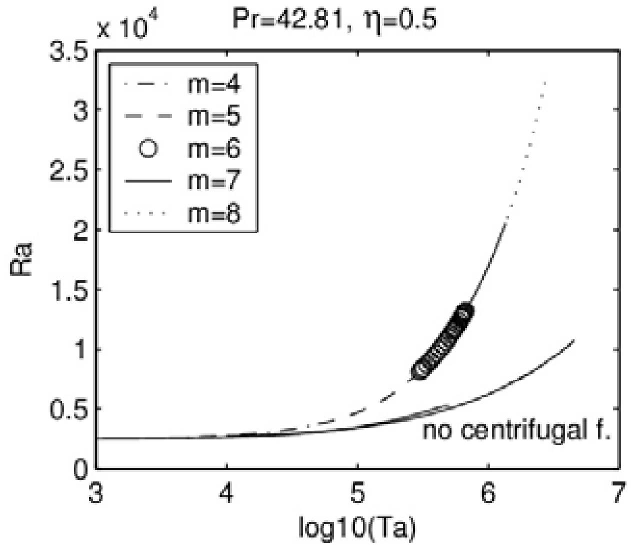

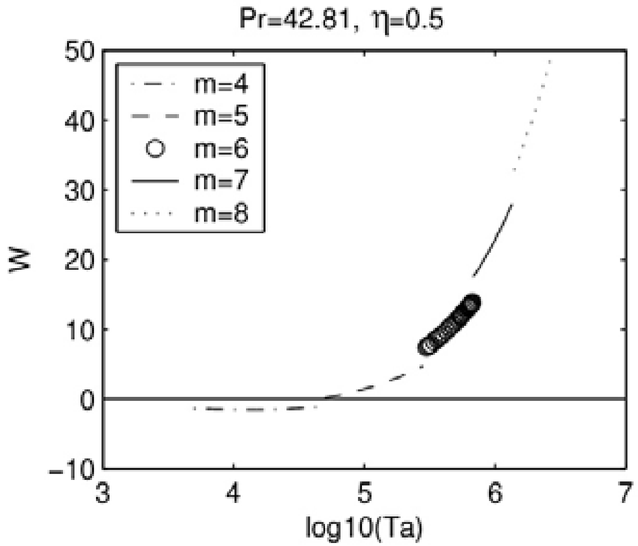

- shape of stability curves nearly independent on *Pr*
- instability due to Hopf bifurcation
- for large *Ta*: $Ra_{centr} \sim Ta^{2/3}$

  [P.H. Roberts, *On the thermal instability of a rotating-fluid sphere containing heat sources*, Philos. Trans. R. Soc. London 263 (1968), 93-117]
- drift velocity W changes sign (slows down or fastens rotation)

Source: Travnikov et al. (2003), Travnikov (2004)

Path-following analysis for stationary solutions at $Ta = 0$

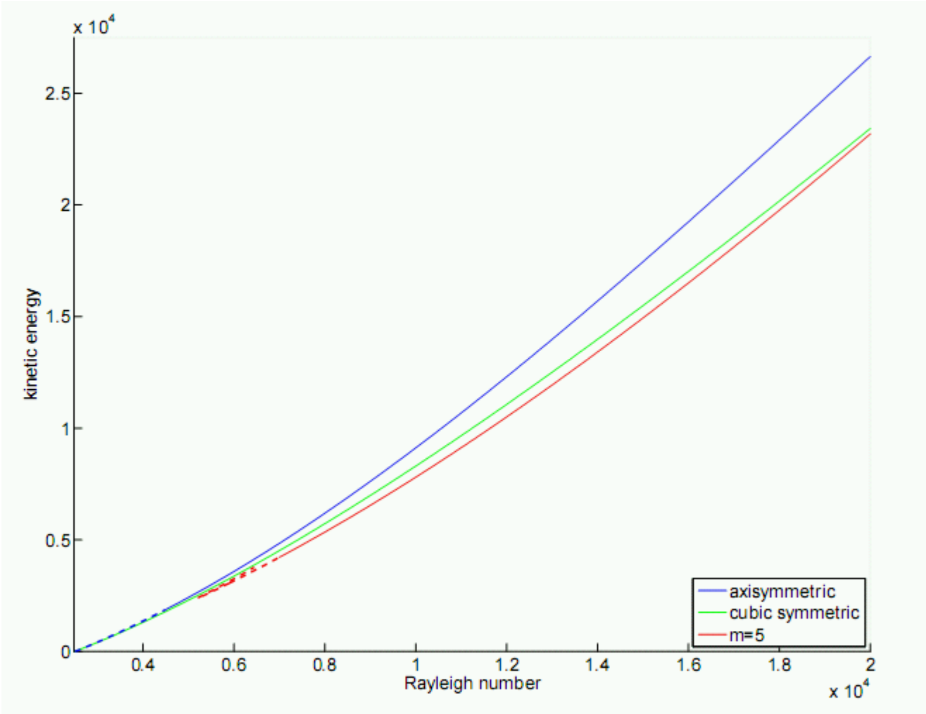

- existence of multistability (axisymmetry, cubic, $m = 5$)
- sudden onset of chaos at $Ra > 28000$
- hysteresis behaviour of the chaotic branch resulting in frozen states with tetrahedral symmetry

Source: K. Bergemann, L. Tuckerman, F. Feudel, *GeoFlow: On symmetry-breaking bifurcations of heated spherical shell convection*, J. Phys.: Conf. Ser. **137** (2008), 012027 (4pp)
K. Bergemann: *Konvektion im Kugelspalt: Numerische Untersuchung und Bifurkationsanalyse am Beispiel des GeoFlow-Experimentes*, Diplomarbeit, Universität Potsdam, 2008

Path-following analysis for stationary solutions at $Ta = 0$

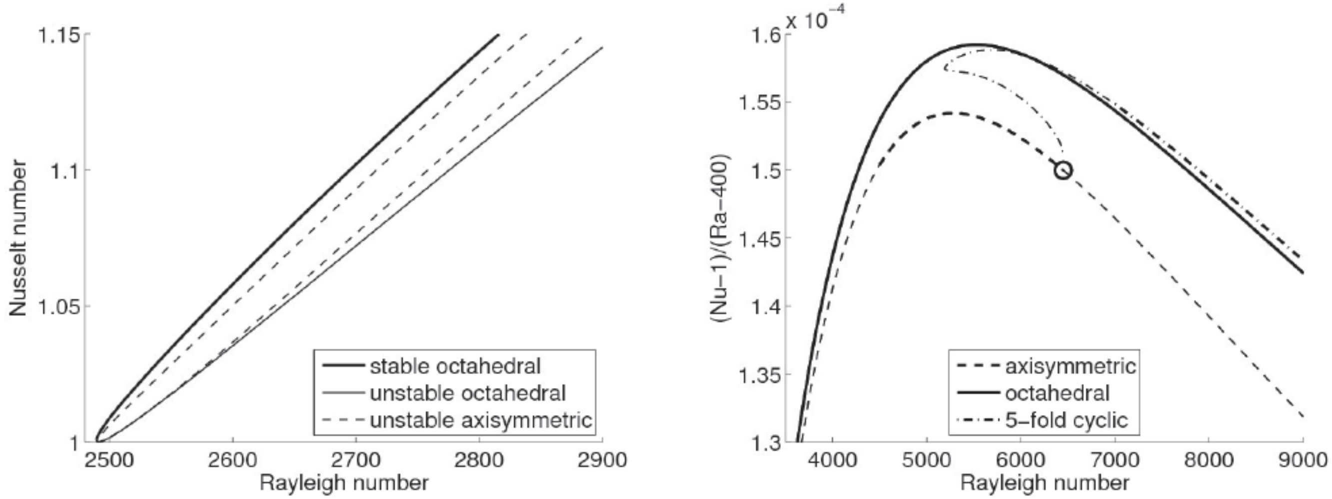

- symmetry breaking bifurcation, with
- an axissymmetric and an cubic symmetric state bifurcate simultaneously
- existence of unstable and stable solutions

Source: K. Bergemann, F. Feudel, C. Egbers, M. Gellert, R. Hollerbach, L. Tuckerman, *Spherical convection - the non-rotating situation revisited,* Topical Team meeting 11.-12. June 2009, Cotbus, unpublished presentation

Global variables for *Ta* low ($Ta \leq 10^4$)

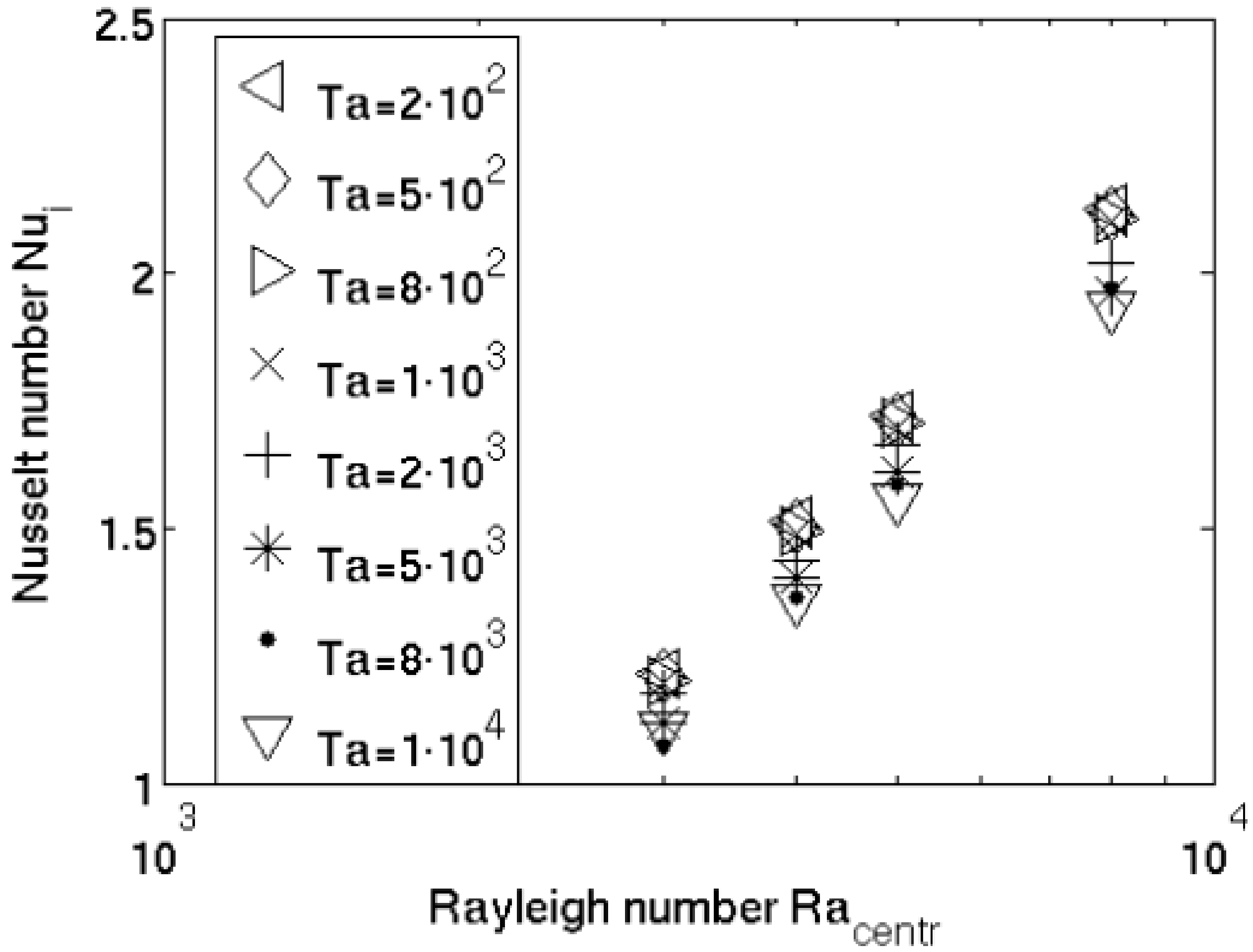

Global variables for Ta low ($Ta \leq 10^4$)

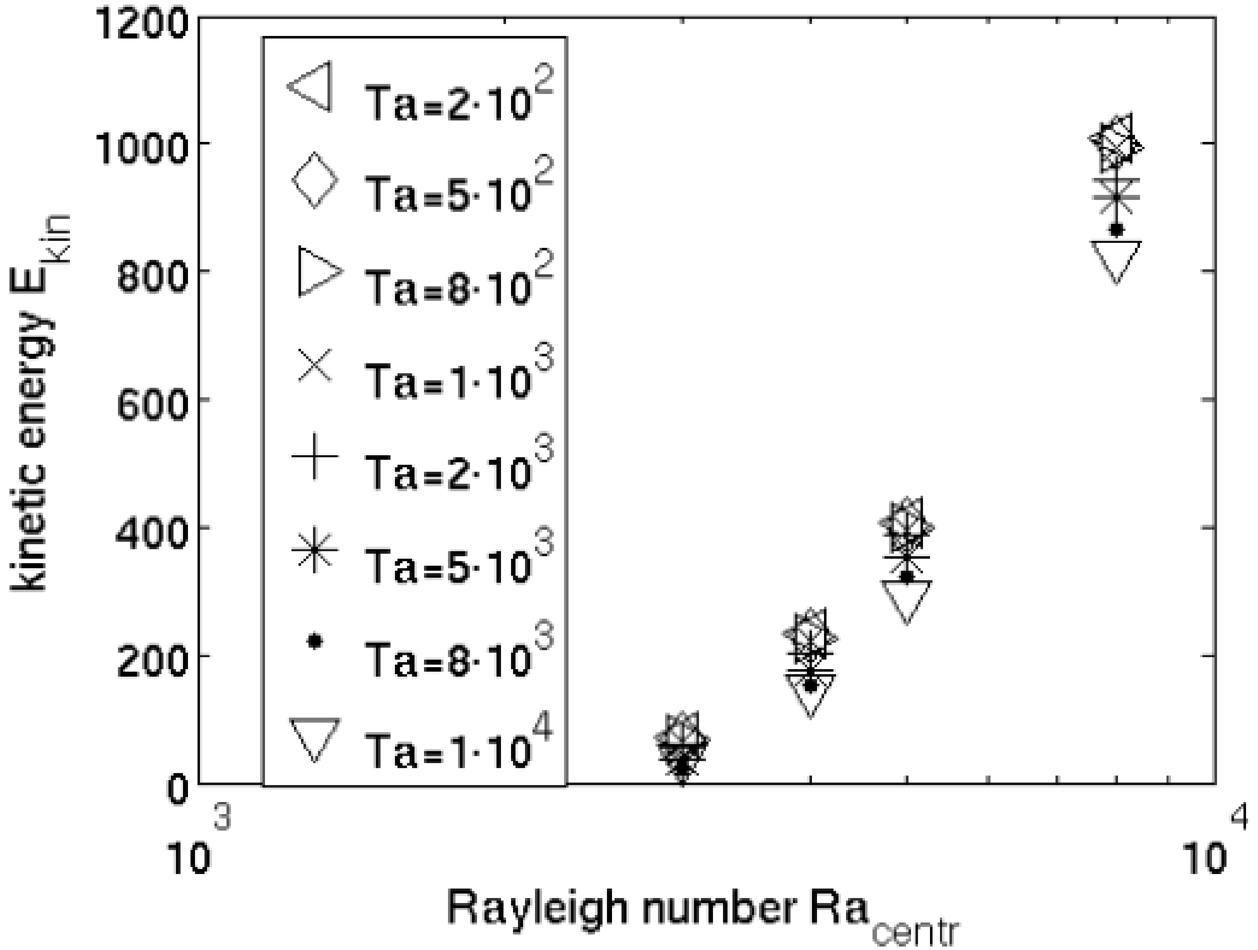

Experiment conditions

- GeoFlow experiment container, integrated in Fluid Science Laboratory (FSL) of COLUMBUS module on ISS
- launch: Feb 7, 2008
- start: Aug 8, 2008
- return: March 2009

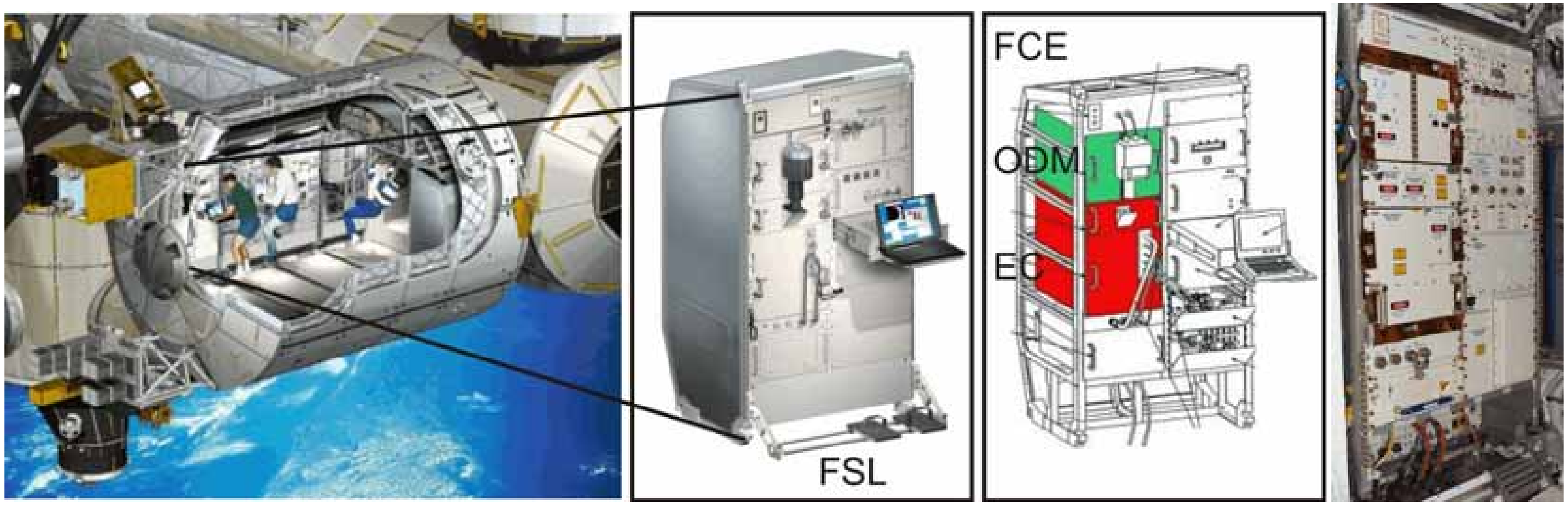

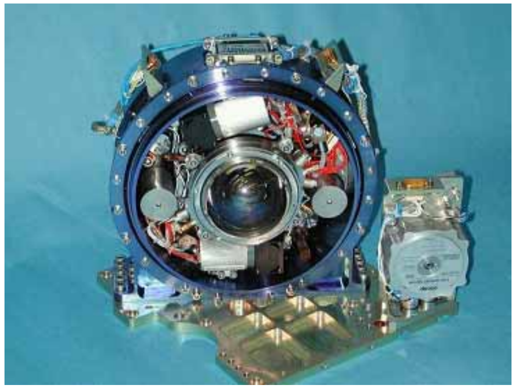

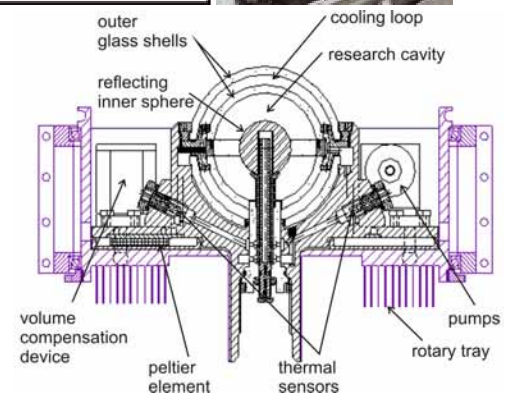

Sources: European Space Agency (ESA); National Aeronautics and Space Administration (NASA); EADS Astrium GmbH, Friedrichshafen

Processing and data transfer from ISS to BTU

Data transfer

ISS $\longleftrightarrow$ BTU

Experimental data: ca. 20s
Image data: ca. 1d

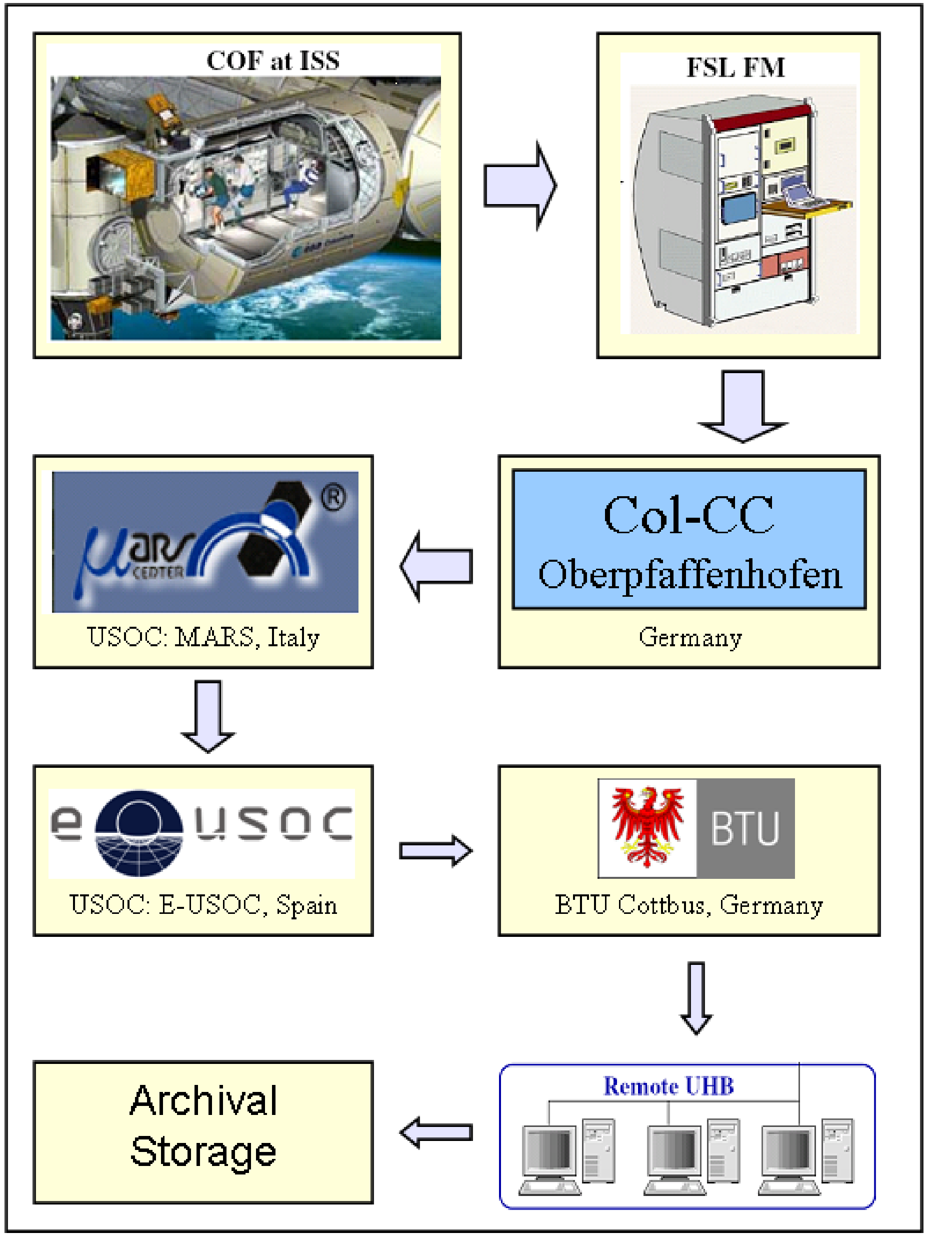

Interferometry: camera position and image view

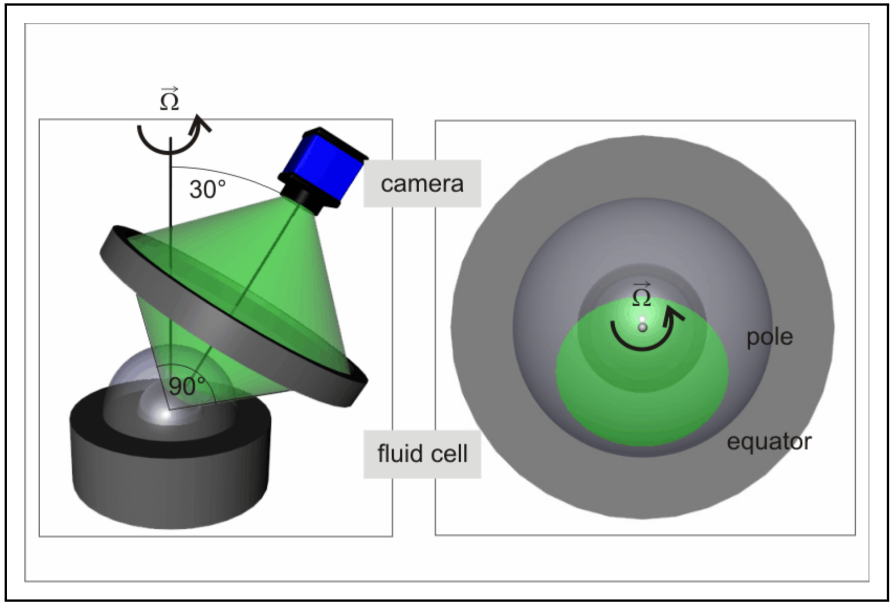

- temperature gradient → density gradient → refractive index gradient → variation of optical path length → interference visualized with Wollaston shearing interferometry
- triggering of image capture each 60° → 6 positions gives measurement picture of whole hemispherical surface

Data volume

images	200 GB
telemetry	50 GB

telemetry - technical values, scientific values (ΔT, μg, etc.)

Dynamics of GeoFlow:
. . . with specific selection for first evaluation: $Ta \neq 0$

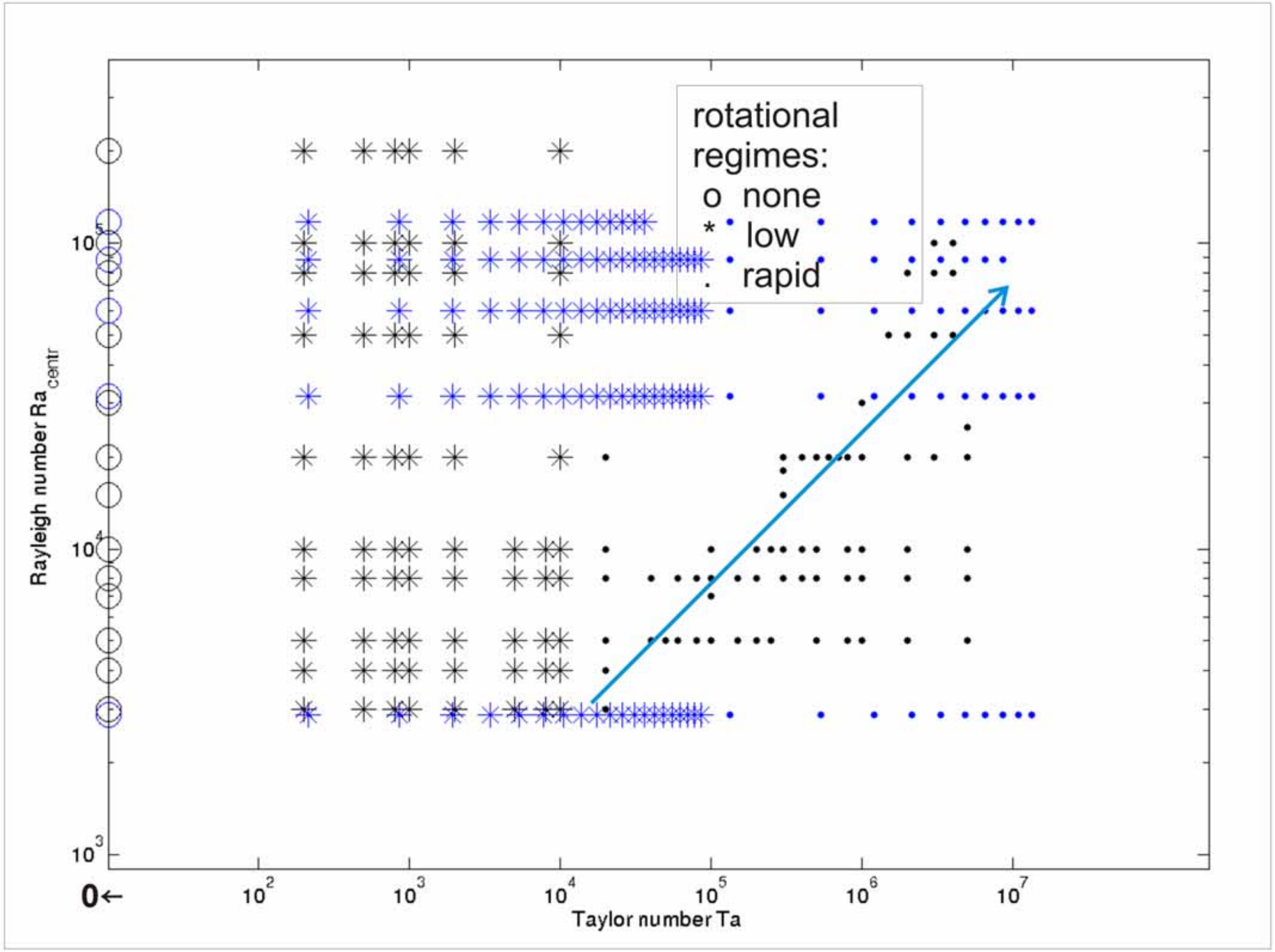

Tracking stability line

Run#5: $(\Delta T_{soll} = 8.2\ K, f_{soll} = 1.8\ Hz)$
$\rightarrow (Ra_{centr,soll} = 1.17349 \cdot 10^5, Ta_{soll} = 1.0876265 \cdot 10^7)$

turn	pos. 0°	60°	120°	180°	240°	300°
1.	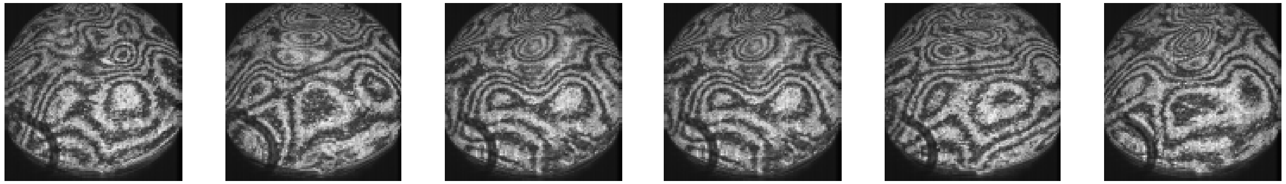					
2.	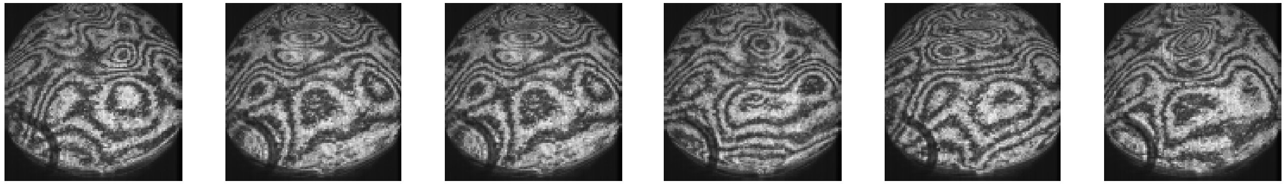					
3.	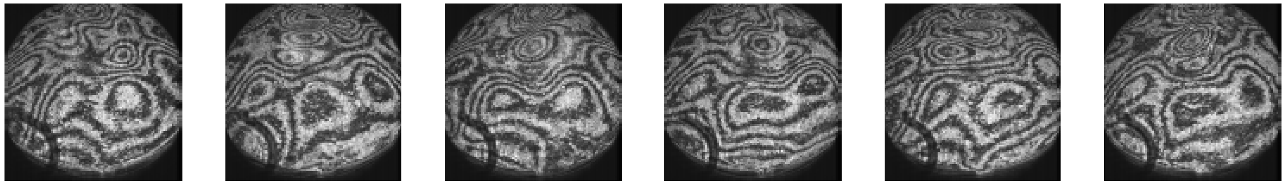					
4.	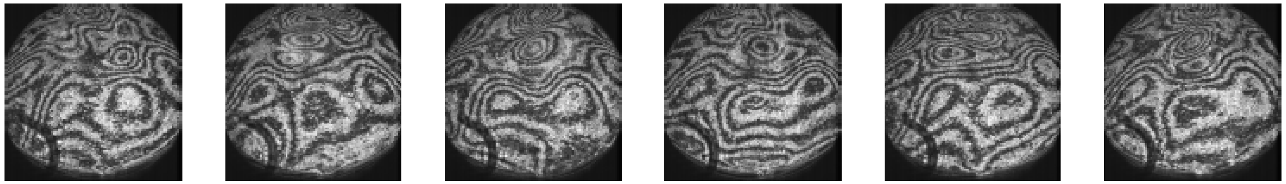					
	0 s	0.093 s	0.860 s	0.279 s	0.372 s	0.465 s
	time t	$\rightarrow$				

Tracking stability line

Run#5: $(\Delta T_{soll} = 8.2\ K, f_{soll} = 2.0\ Hz)$
$\rightarrow (Ra_{centr,soll} = 1.17349 \cdot 10^5, Ta_{soll} = 1.3427488 \cdot 10^7)$

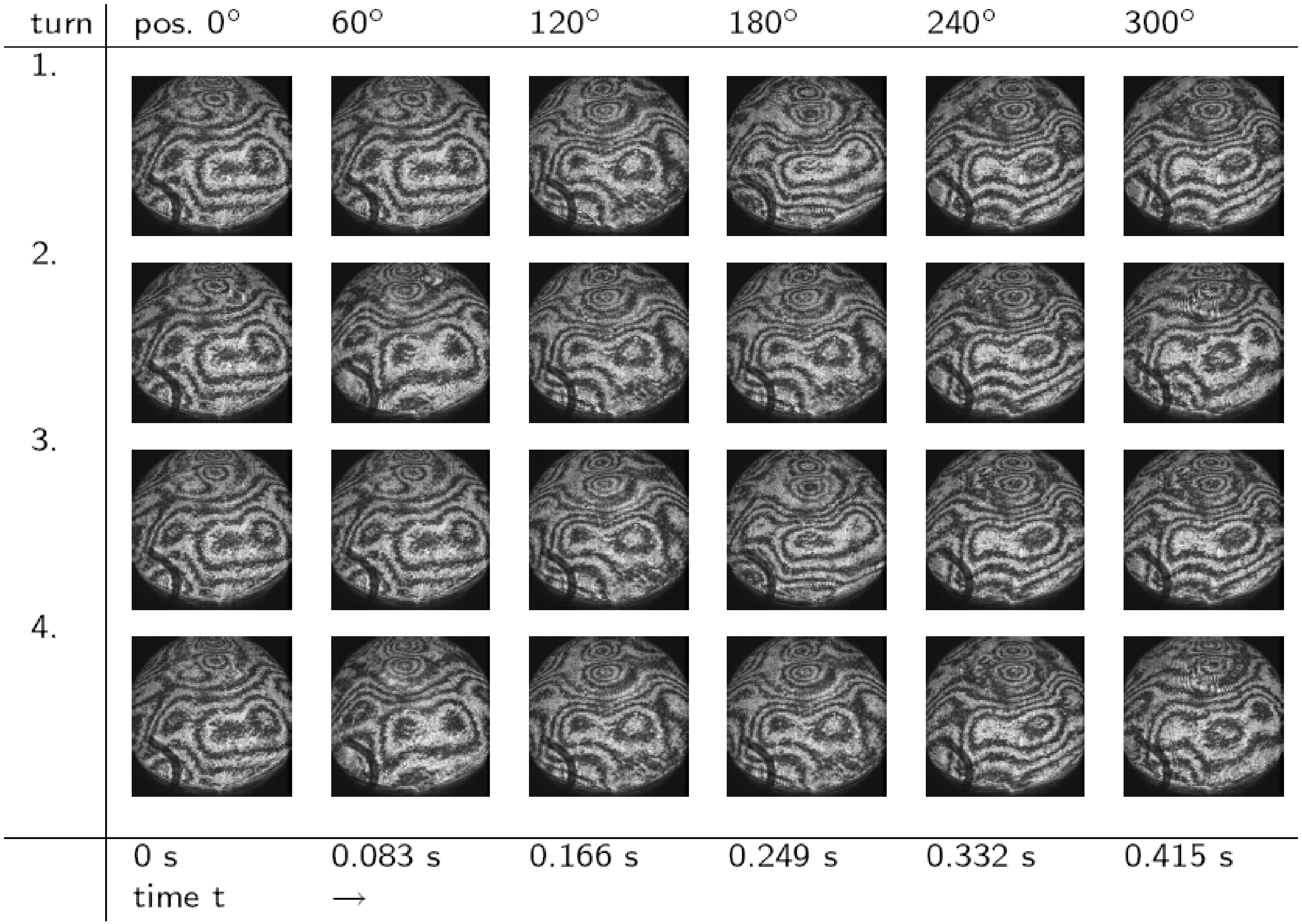

Dynamics of GeoFlow:
...with specific selection for first evaluation: $Ta = 0$

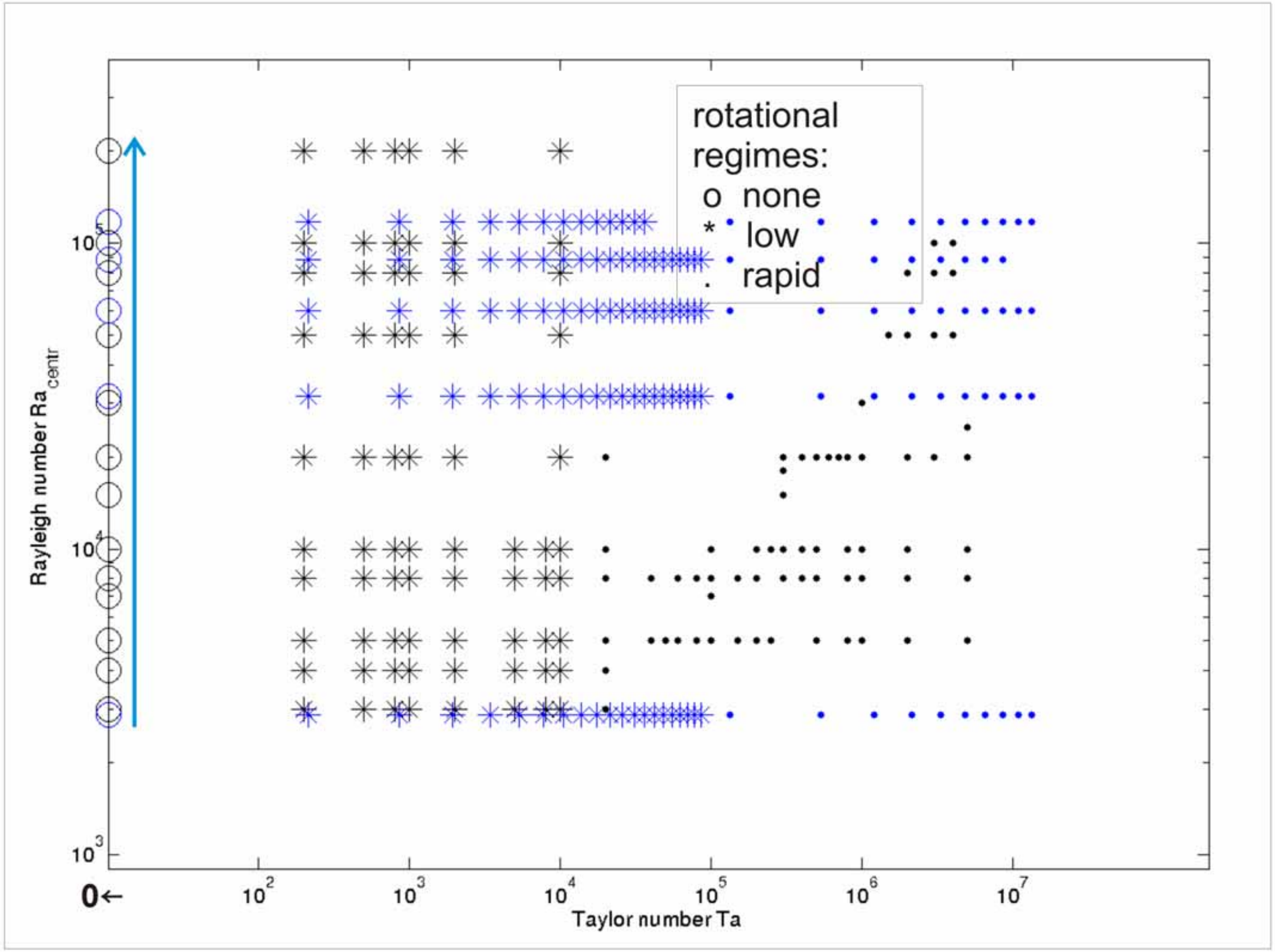

Octahedral solution and its appearance in fringes

Pattern of convection by visualization of temperature field in radial direction with view at the top of the sphere, i.e. the middle of the image is the 'polar' region. Isolines demonstrate character of the pattern, captured by interferometry. Dark shading shows hot up-flow:

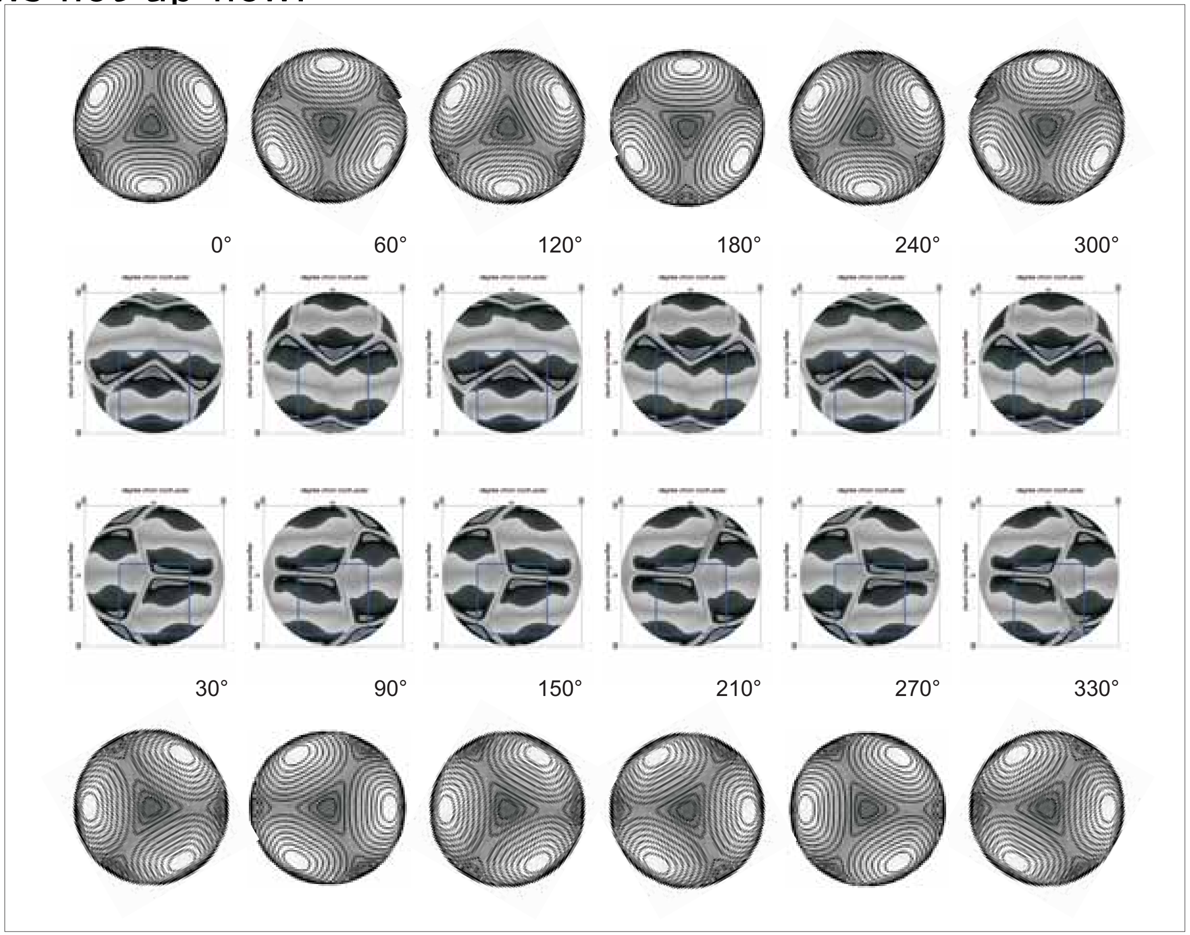

fringe pattern

- topology at the polar region, partly outreaching to equator
- shows a repetition of patterns every second position

Tracking stable solution

Run#2: $\Delta T_{soll} = 2.2\ K,\ Ra_{centr,soll} = 3.15 \cdot 10^4$

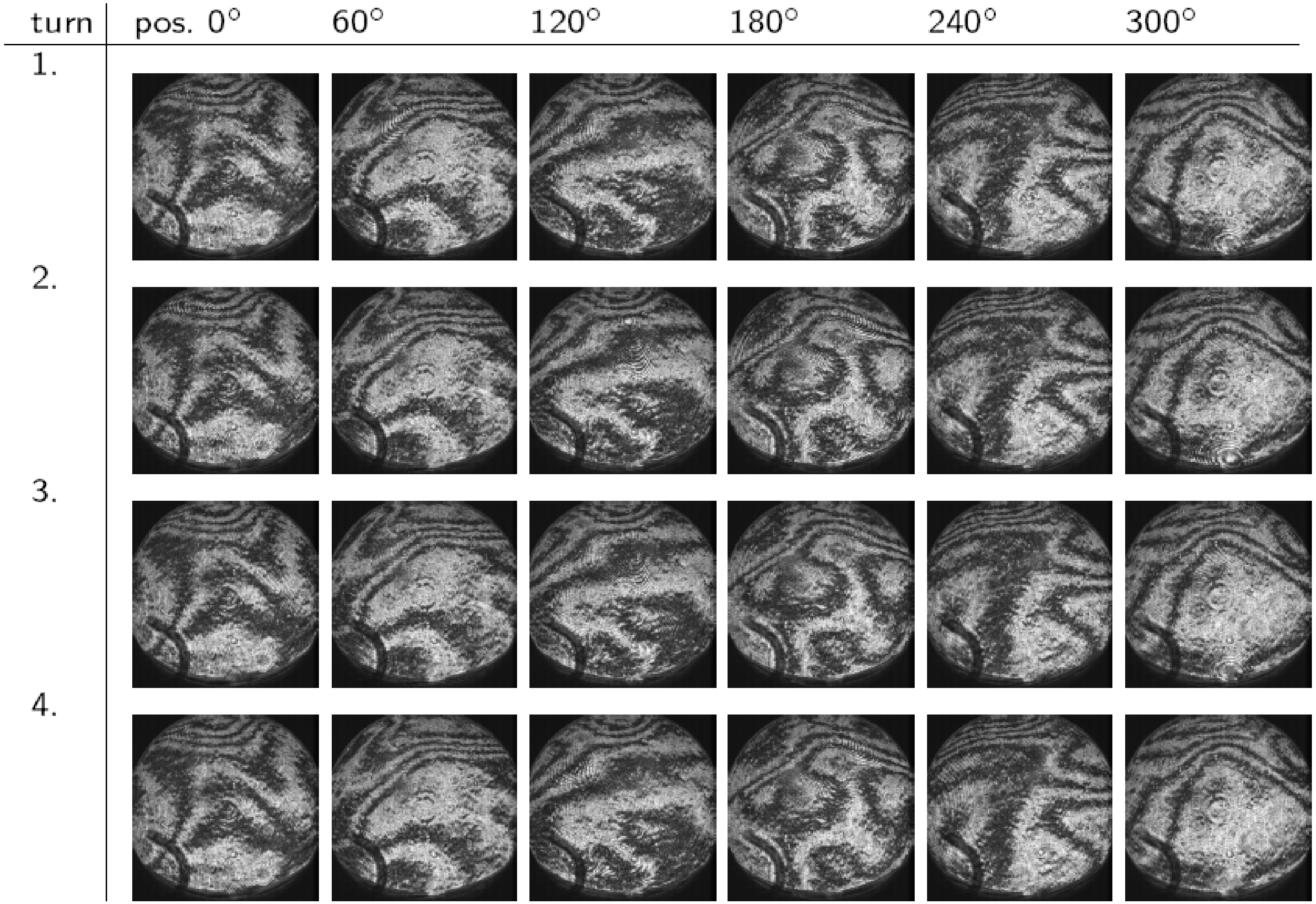

Process of reconstruction of whole hemisphere in a plane

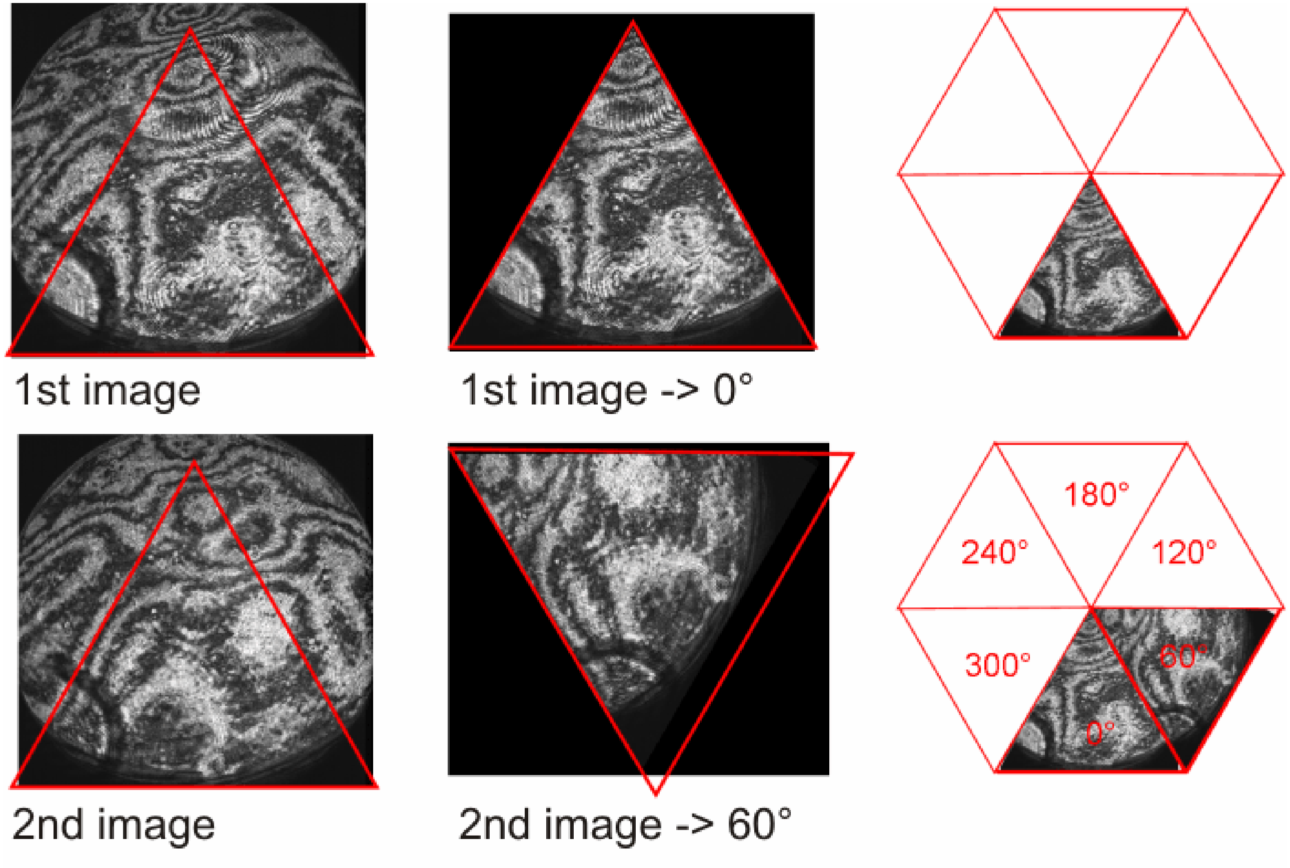

- image taken every 60° $\longrightarrow$ images overlap $\longrightarrow$ only a sector is visible
- defined mask (ROI) over image sequence $\longrightarrow$ 6 sectors
- note: no interpolation, because of mixing fringes to gray
- note: pole is supposed to be fixed

Reconstruction of images for specific part during RUN #4

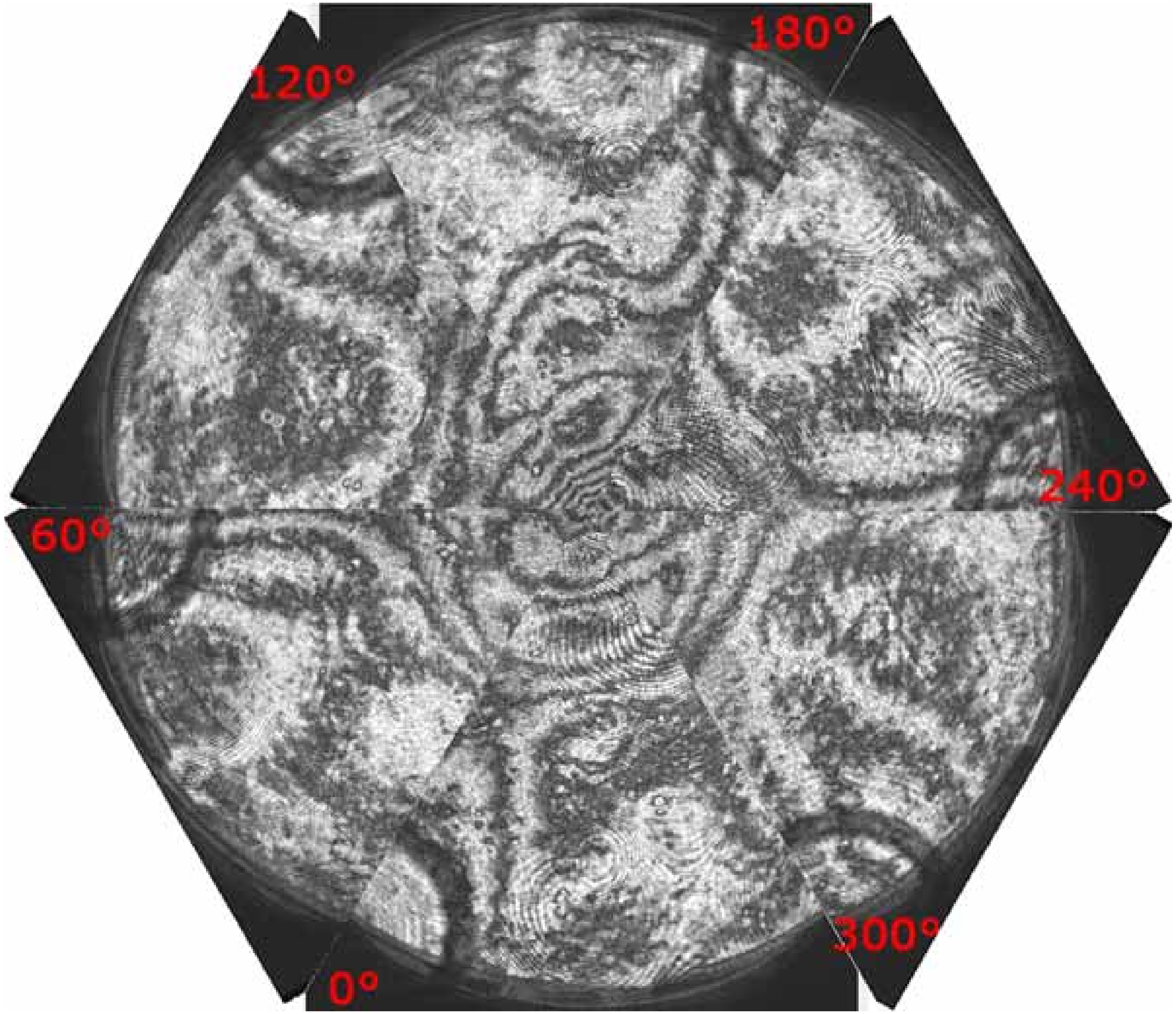

Parameter Regime with numerical and experimental data base

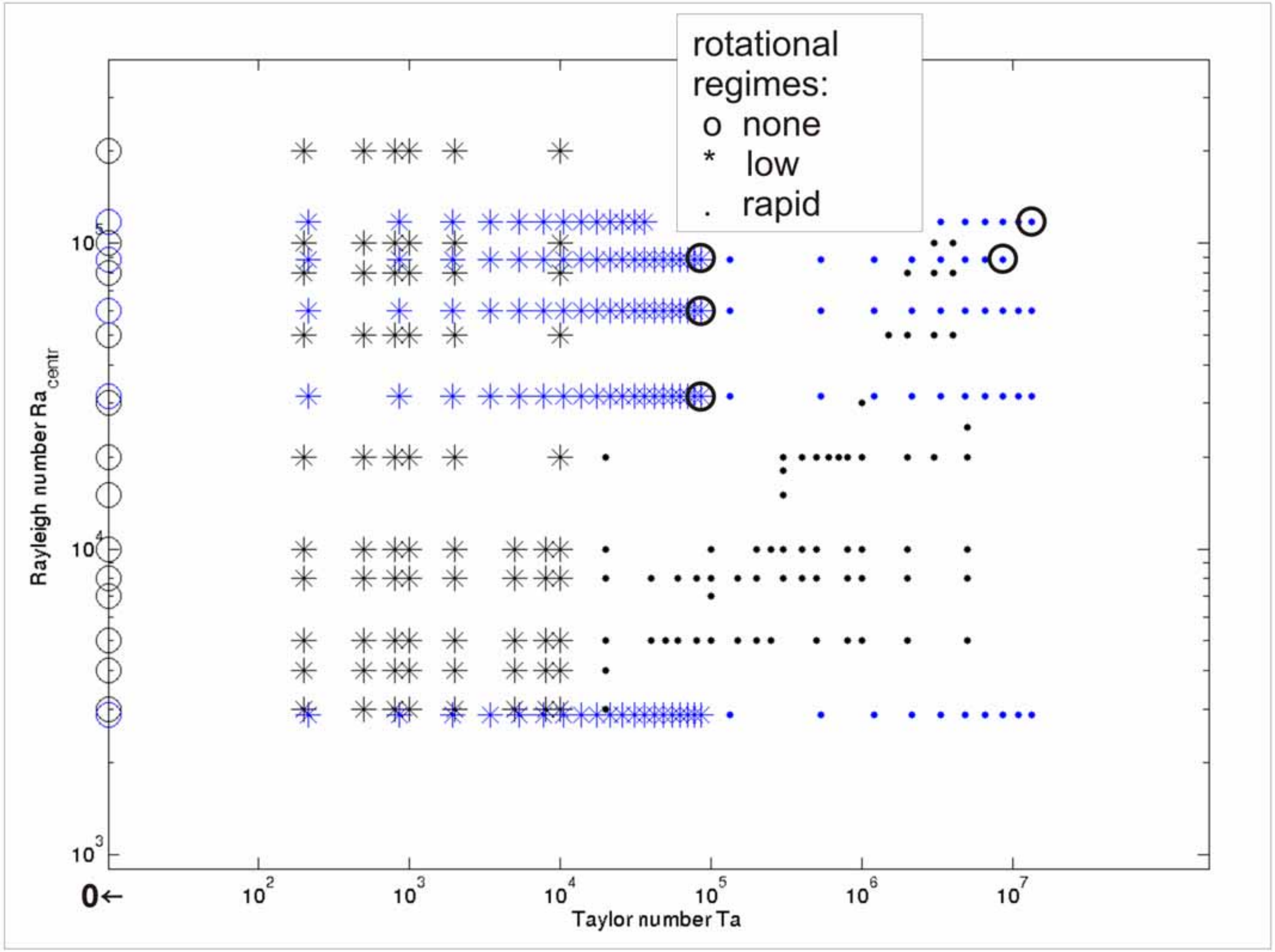

Patterns of convection in the rapid rotation regime: Alignment of convective cells at the tangent cylinder

$Ra_{centr} = 8.87 \cdot 10^4$
$Ta = 8.59 \cdot 10^6$

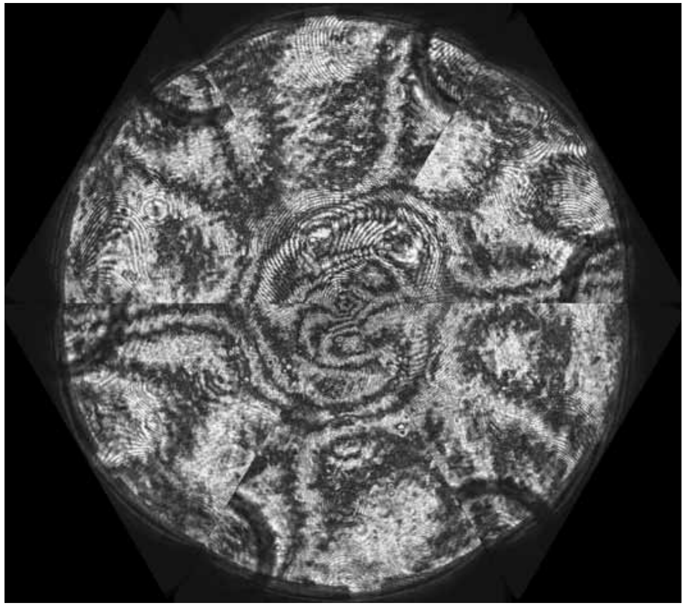

$Ra_{centr} = 1.17 \cdot 10^5$
$Ta = 1.34 \cdot 10^7$

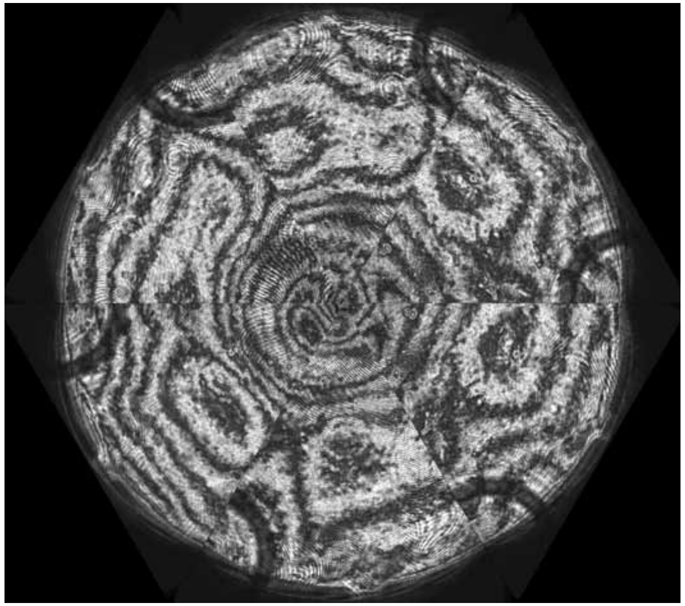

'columnar cells'

Patterns of convection in the moderate rotation regime: Increase of thermal forcing leads to symmetry breaking bifurcations

$Ra_{centr} = 3.15 \cdot 10^4$
$Ta = 8.59 \cdot 10^4$

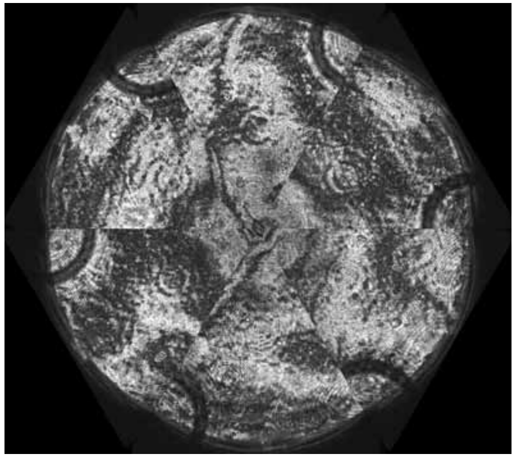

$Ra_{centr} = 6.01 \cdot 10^4$
$Ta = 8.59 \cdot 10^4$

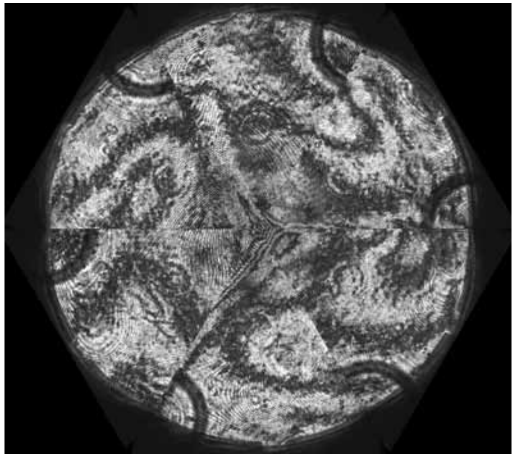

$Ra_{centr} = 8.87 \cdot 10^4$
$Ta = 8.59 \cdot 10^4$

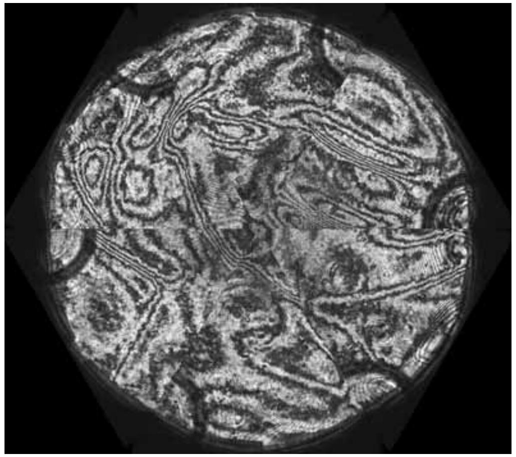

Alignment for single image: Identification of fringe pattern as ‘columnar cells’

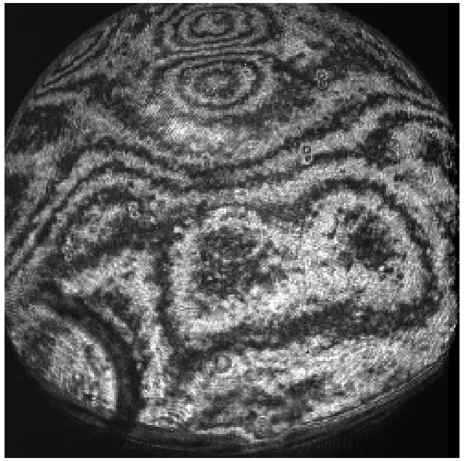

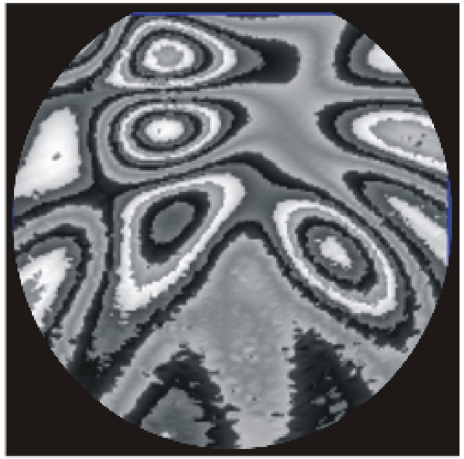

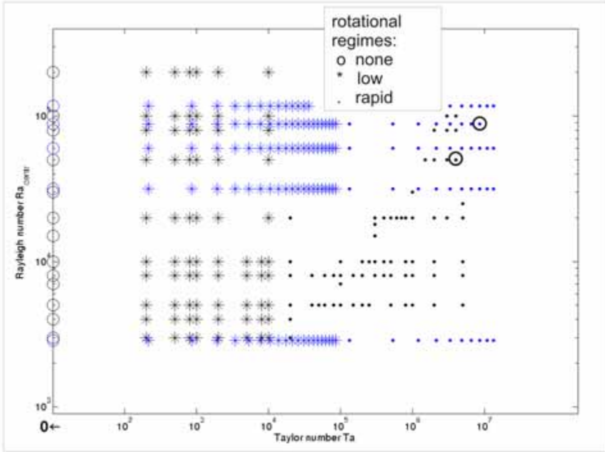

	experimental	numerical
Ra_{centr}	$9 \cdot 10^4$	$5 \cdot 10^4$
Ta	$9 \cdot 10^6$	$4 \cdot 10^6$

$\rightarrow$ shift between experimental and numerical stability regimes

Summary

- GeoFlow
  - spherical Rayleigh-Bénard convection experiment in self-gravitating force field
  - microgravity environment of COLUMBUS on ISS
  - superposition of rotation
- dynamics for
  - non-rotating case
    - coexisting of several modes (axisymmetric, cubic, pentagonal)
    - influence of initial conditions to reach different stable states
    - transition from steady to irregular flow with remnant tetrahedral symmetry
  - rotating case
    - complex pattern drift
    - transition to stabilizing effects due to centrifugal forces
    - transition from steady via periodic to irregular flow
- first evaluated experimental images show numerically presumed dynamics and
  - for the non-rotating case: octahedral, stationary solution
  - for the rotating case: stability line